Environmental Pollution 332 (2023) 121926

Contents lists available at ScienceDirect

Environmental Pollution

journal homepage: www.elsevier.com/locate/envpol

Dissolved gaseous mercury production and sea-air gaseous exchange in impacted coastal environments of the northern Adriatic Sea☆

Federico Floreani [a,b,*], Nicolò Barago [a], Katja Klun [c], Jadran Faganeli [c], Stefano Covelli [a]

[a] Department of Mathematics & Geosciences, University of Trieste, Via E. Weiss 2, 34128, Trieste, Italy
[b] Department of Life Sciences, University of Trieste, Via L. Giorgieri 5, 34127, Trieste, Italy
[c] Marine Biology Station, National Institute of Biology, Fornace 41, 6330, Piran, Slovenia

ARTICLE INFO

Keywords:
Idrija mercury mine
Mercury evasion
Fish farm
Flux chamber
Water-air exchange

ABSTRACT

The northern Adriatic Sea is well known for mercury (Hg) contamination mainly due to historical Hg mining which took place in Idrija (Slovenia). The formation of dissolved gaseous mercury (DGM) and its subsequent volatilisation can reduce the amount of Hg available in the water column. In this work, the diurnal patterns of both DGM production and gaseous elemental Hg (Hg^0) fluxes at the water-air interface were seasonally evaluated in two selected environments within this area, a highly Hg-impacted, confined fish farm (VN: Val Noghera, Italy) and an open coastal zone less impacted by Hg inputs (PR: Bay of Piran, Slovenia). A floating flux chamber coupled with a real-time Hg^0 analyser was used for flux estimation in parallel with DGM concentrations determination through in-field incubations. Substantial DGM production was observed at VN (range = 126.0–711.3 pg L^{-1}) driven by both strong photoreduction and possibly dark biotic reduction, resulting in higher values in spring and summer and comparable concentrations throughout both day and night. Significantly lower DGM was observed at PR (range = 21.8–183.4 pg L^{-1}). Surprisingly, comparable Hg^0 fluxes were found at the two sites (range VN = 7.43–41.17 ng m^{-2} h^{-1}, PR = 0–81.49 ng m^{-2} h^{-1}), likely due to enhanced gaseous exchanges at PR thanks to high water turbulence and to the strong limitation of evasion at VN by water stagnation and expected high DGM oxidation in saltwater. Slight differences between the temporal variation of DGM and fluxes indicate that Hg evasion is more controlled by factors such as water temperature and mixing conditions than DGM concentrations alone. The relative low Hg losses through volatilisation at VN (2.4–4.6% of total Hg) further confirm that static conditions in saltwater environments negatively affect the ability of this process in reducing the amount of Hg retained in the water column, therefore potentially leading to a greater availability for methylation and trophic transfer.

1. Introduction

Mercury (Hg) is a toxic element which occurs naturally under different inorganic and organic forms in every environmental compartment, at least at relatively low concentrations (Beckers and Rinklebe, 2017). A peculiarity of this metal is the high vapour pressure and low solubility of its elemental form, often referred to as gaseous elemental mercury (Hg^0 or GEM). This specie usually represents more than 90% of the Hg occurring in the atmosphere and can persist for more than 1 year in this compartment (Ariya et al., 2015; Ren et al., 2016; Saiz-Lopez et al., 2018). This long residence time allows Hg^0 to be subject to long-range atmospheric transport before being removed through dry or wet depositions mostly after oxidation to the more soluble ionic form (Hg^{2+}) (Ariya et al., 2015; Custodio et al., 2020; Zhang et al., 2012). Moreover, after deposition, Hg^{2+} can be reduced to Hg^0 and re-emitted into the atmosphere, further enhancing its dispersion throughout the environment (Fitzgerald et al., 1998; Strode et al., 2007; Zheng and Hintelmann, 2009). Historical emissions related to various anthropogenic activities (e.g. mining, coal combustion, metal production, …(UN Environment, 2019)) have contributed to significantly increase the amount of Hg involved in these exchanges compared to pre-industrial levels (Enrico et al., 2017; Mason and Sheu, 2002). As a result, Hg pollution has been recognised as a global concern by the Minamata Convention in 2013 (Selin et al., 2018).

☆ This paper has been recommended for acceptance by Dr Michael Bank.

* Corresponding author. Department of Mathematics and Geosciences University of Trieste Via E. Weiss 2, 34128, Trieste, Italy.
E-mail address: federico.floreani@phd.units.it (F. Floreani).

https://doi.org/10.1016/j.envpol.2023.121926
Received 27 February 2023; Received in revised form 9 May 2023; Accepted 28 May 2023
Available online 31 May 2023

Aquatic ecosystems are particularly sensitive to Hg pollution due to the possible conversion of inorganic Hg to the organic form methylmercury (MeHg), which can be easily bioaccumulated and biomagnified in food webs and can have notable toxic effects on biota and humans mainly on the nervous system (Díez, 2009; Morel et al., 1998). MeHg is mainly produced in anoxic sediments and water layers by several microorganisms (Fitzgerald et al., 2007; Parks et al., 2013), although several pathways for Hg methylation, even in oxic water layers, have recently been identified (Wang et al., 2022). Moreover, coastal and marginal sea environments are considered more vulnerable to Hg pollution as they represent hot spots for Hg methylation due to both the high Hg loadings related to both atmospheric depositions and direct riverine inputs (Amos et al., 2014; Kotnik et al., 2015; Xue et al., 2019) and the high nutrient concentrations along with rates of microbial activity (Hammerschmidt and Fitzgerald, 2004). The formation of Hg^0 and subsequent evasion at the water-air interface can represent a relevant pathway for reducing the amount of Hg^{2+} available for methylation into the aquatic environment (Horvat et al., 2003). Considering that Hg^0 is the largely predominant constituent of the volatile Hg fraction in water, with volatile organic dimethylmercury (DMeHg) occurring only at extremely low concentrations in deep water layers and rarely detected in surface waters (Black et al., 2009; Cossa et al., 2009; Kotnik et al., 2017), hereafter it will be referred to as DGM (Dissolved Gaseous Mercury), commonly used to indicate the operationally defined gaseous Hg fraction in water. In surface seawater, DGM is produced through abiotic (photochemical) and biotic reduction of Hg^{2+} (Amyot et al., 1997; Kuss et al., 2015; Qureshi et al., 2010), with photoreduction considered the dominant pathway due to its higher rates (Soerensen et al., 2010). An important control on photoreduction rates is exerted by dissolved organic matter (DOM), which, depending on its concentration and structure, can: i) promote reaction rates acting as a photosensitiser, particularly if it is rich in chromophores (Costa and Liss, 1999; Fantozzi et al., 2007), ii) form strong complexes with Hg^{2+} due to its high affinity for reduced sulphur groups (e.g. thiols), rendering it non-photoreducible (O'Driscoll et al., 2018), iii) reduce light penetration through the water column and the efficacy of photochemical reactions (Castelle et al., 2009). Moreover, DGM can be produced even in the absence of light through "dark reduction" reactions mediated by microbial activity (Fantozzi et al., 2009) or by interaction with a particular fraction of organic matter (OM) e.g. humic substances (Allard and Arsenie, 1991). These processes are generally more important in deep water layers and sediments (Amyot et al., 1997; Lepak et al., 2021). However, DGM in water can be re-oxidised to non-volatile Hg^{2+} mainly through photochemical reactions occurring at the same time as photoreduction (Whalin et al., 2007) and enhanced in saltwater environments by the presence of halides (e.g. Cl^-, Br^-) (Ci et al., 2016). When the balance between production through reduction and losses through oxidation leads to a super-saturation of DGM in surface water, evasion into the atmosphere can take place (Southworth et al., 2007) as a function of both DGM availability and physical forcing such as temperature, water

Fig. 1. Study area and sampling sites (satellite images from Bing).

turbulence, mixing or currents (Lindberg and Zhang, 2000; Sharif et al., 2013).

The northernmost part of the Adriatic Sea (Gulf of Trieste, Italy) is one of the coastal marine areas most impacted by anthropogenic releases of Hg in the world (Fitzgerald et al., 2007). The main source of Hg in this area is the transport of Hg-enriched sedimentary material by the Isonzo River as a consequence of the dispersion into the environment of large amounts of this element (>35,000 t; Dizdarevič, 2001; Gosar et al., 1997) due to historical cinnabar mining in Idrija (Slovenia) which lasted for approximately 500 years (Covelli et al., 2001). As a result of the erosion and leaching of contaminated surfaces, the Isonzo River still carries notable amounts of Hg into the Gulf of Trieste, even 25 years after the mine closure, mostly after intense rain events (Covelli et al., 2007; Baptista-Salazar et al., 2017). At the mouth of the Isonzo River, the contaminated material is diverted westward by the prevalent anticlockwise water circulation of the Gulf and enters the Marano and Grado Lagoon, where Hg can accumulate in sediments mainly in the eastern sector (Acquavita et al., 2012). A second anthropogenic source of Hg is related to past uncontrolled discharges from the 1940s to the 1980s of processing and seepage wastewaters from a chlor-alkali plant (Torviscosa, Italy) into the Aussa River and consequently into the lagoon (Covelli et al., 2009). Mercury contamination of this lagoon is of particular concern considering that traditional aquaculture in the form of fish farms cover approximately 14% of its area (Acquavita et al., 2015). These fish farms are closed environments, isolated from the rest of the lagoon by man-made embankments, having only limited water exchanges with the external lagoon (Petranich et al., 2018a). As a consequence of scarce water dynamics, notable OM inputs and occurrence of anoxic conditions (mostly during summer), remarkable Hg methylation and bioaccumulation through the trophic web can be observed in this kind of environments (Bettoso et al., 2023; Petranich et al., 2018b).

Understanding the processes that control Hg speciation and gaseous exchanges at the water-air interface in coastal areas subject to considerable Hg supplies related to anthropogenic activities is of particular interest in order to evaluate the ability of gaseous exchanges to reduce the burden of Hg available to methylation and trophic transfer, mostly in environments characterised by limited water exchanges. In-depth knowledge of these processes may also be useful to better assess the impact of Hg pollution on ecosystems and human health, also helping define possible mitigation strategies (Bouchet et al., 2011; Clarke et al., 2023; Hsu-Kim et al., 2018). At present, only limited information exists regarding Hg^0 exchanges at the water-air interface in the highly Hg impacted northernmost part of the Adriatic Sea (Floreani et al., 2019). In the cited study, Hg^0 fluxes were measured in 4 sites within this area, specifically two located inside a fish-farm of the Marano and Grado Lagoon (Val Noghera fish farm), one in the open lagoon environment and one in a *quasi*-pristine open coastal zone of the Gulf of Trieste (the Bay of Piran, Slovenia) less subjected to riverine Hg inputs. Measurements conducted inside the fish farm showed Hg^0 fluxes lower than those obtained in the open lagoon environment and comparable to those found in the less contaminated area of Piran. However, these results were referred only to diurnal period. In this study, DGM concentrations and Hg^0 fluxes over the entire daily cycle (24 h) were evaluated in different seasons in two previously monitored sites (Floreani et al., 2019). The first is located in the highly impacted area of Val Noghera fish farm (VN, Lat 45°42′48.95″N, Long 13°17′17.03″E), characterised by scarce water exchange, whereas the second site is located in the *quasi*-pristine and more hydrodynamic coastal area of the Bay of Piran (PR, Lat 45°31′06.00″N, Long 13°34′04.65″E). Site selection was aimed at verifying possible differences in factors influencing DGM production and volatilisation in two markedly different environmental contexts commonly occurring within the contaminated area of the Northern Adriatic Sea in terms of hydrodynamics and Hg contamination degree. The expected results will also be helpful to assess the effectiveness of gaseous exchanges in limiting the burden of Hg available in the water column.

2. Materials and methods

2.1. Environmental settings

The Val Noghera fish farm is located in the central part of the Marano and Grado Lagoon (Northern Adriatic Sea, Italy), one of the best preserved wetland transitional environments in the entire Mediterranean area, covering an area of approximately 160 km^2 between the Tagliamento and Isonzo River deltas (Fig. 1). The Val Noghera fish farm extends over a total area of 2.7 km^2, most of which is occupied by shallow waters and saltmarshes, having become a habitat for many bird species, and is characterised by extremely limited water recycling and recirculation. More details about the hydrogeology and management of these environments have been reported in previous works (Petranich et al., 2018a, 2018b). Our sampling site (VN) is located in a channel of the older sector of the fish farm, characterised by a relatively shallow water column (~2 m) and Hg concentrations in sediments ranging between 2.15 and 5.10 mg kg^{-1} (Petranich et al., 2018b).

The Bay of Piran is a semi-enclosed area located in the southern part of the Gulf of Trieste, close to the border between Slovenia and Croatia (Fig. 1), and covers an area of approximately 19 km^2. It is a typical marine area with a maximum depth of ~15 m, influenced by the irregular supply of freshwater from the Dragonja River to its inner sector, with an average discharge of 4 m^3 s^{-1} (Cozzi et al., 2012; Ogorelec et al., 1991; Pavoni et al., 2020). Thanks to the limited Hg supplies from the northern part of the Gulf, the concentrations of this metal reported for sediments of the bay are relatively low (<0.5 mg kg^{-1}, Covelli et al., 2001; Faganeli et al., 1991). Measurements at this site (PR) were performed in the northern part of the bay near the local Marine Biology Station.

The climate of the area can be defined as oceanic mesotemperate (Pesaresi et al., 2014) with relatively warm temperatures throughout the entire year with occasional droughts in summer. Sea breezes blowing from the north-east during the night and morning (2–3 m s^{-1}) and from the sea in the afternoon (3–4 m s^{-1}) strongly affect the temperature regime (ARPAFVG-OSMER, 2014) together with the irregular occurrence of a strong north-easterly Bora wind, mostly during winter (Boldrin et al., 2009). The highest water temperatures are observed in July, reaching values above 30 °C inside the lagoon (Ferrarin et al., 2010).

2.2. Sampling strategy

Three distinct sampling campaigns to determine Hg^0 fluxes at the water-air interface were performed for both sites during the period of the year characterised by higher irradiation and temperature, which may favour the gaseous exchanges of Hg between the aquatic and atmospheric compartment (Cizdziel et al., 2019; Ferrara et al., 2000; Nerentorp Mastromonaco et al., 2017). More specifically, measurements were performed during late spring (VN: May 2022; PR: June 2021), summer (VN: August 2020; PR: August 2019), and autumn (VN: November 2020, PR: November 2021), whereas no measurements were carried out in winter due to logistical difficulties; however, previously published data report that Hg^0 emission during the winter period in these sites might be relatively low compared to those observed in other seasons (Floreani et al., 2019). The variation of Hg^0 fluxes during the entire 24 h period was assessed by means of a floating flux chamber (FC), taking 11 to 14 distinct sets of measurements at regular time intervals of ~2 h during each sampling campaign. It was, however, sometimes necessary to lengthen this time interval at the Piran site due to the relatively high wave motion observed *in situ*, a condition not optimal for

the application of the adopted experimental approach (Bagnato et al., 2013; Fantozzi et al., 2007).

Continuous measurements of incident UV radiation in the wavelength band between 250 and 400 nm, recognised as the most effective in promoting Hg photoreduction (Amyot et al., 1997; Lee et al., 2019; Qureshi et al., 2010), were conducted using a specific sensor (SU-420, Apogee Instruments, Logan, UT, USA) installed at a height of ~2 m near sampling points in unshaded areas. The sensor has a resolution of 0.1 W m^{-2} and recorded 1 data per minute as an average of the value of the readings taken every 1 s. Average UV intensity, corresponding exactly to the duration of every single flux measurement, was then calculated. Air temperature and relative humidity were monitored in the field through a portable thermohygrometer (HI9565, Hanna Instruments, Padova, Italy).

The main physico-chemical parameters of the surface water layer (temperature, pH, oxidation-reduction potential (ORP), conductivity, salinity, and dissolved oxygen (DO_2)) were monitored in parallel with Hg^0 flux measurements by means of a portable multiprobe meter (HI98194, Hanna Instruments, Padova, Italy).

After each flux measurement, surface water samples were collected for the determination of DOC, total dissolved Hg (THg_D), and DGM concentrations. Aliquots for the determination of DOC (V = 5 mL) were filtered through pre-combusted (450 °C) glass microfiber filters (Whatman GF/F, 0.8 μm pore size) and collected in glass containers. Conversely, mixed cellulose ester membrane filters (Millipore Millex HA, 0.45 μm pore size) were used to collect water samples for THg_D analysis (V = 100 mL) in borosilicate bottles previously conditioned with HCl (2% v/v), rinsed with deionised water (MilliQ) and ignited (60 °C).Samples for THg_D analysis were then immediately oxidised through the addition of 0.5 mL of bromine chloride (BrCl). All samples were stored in the dark and transported to the laboratory, where the aliquots for THg_D were stored at 4 °C, whereas aliquots for DOC determination were frozen until analysed. For each sampling campaign at both sites, three blank samples (MilliQ water) prepared and stored in the same way of real samples were analysed, resulting in values lower than the instrument LOD. Finally, DGM concentrations were determined following incubation in the field of 1 L unfiltered water samples as reported hereafter.

2.3. Analytical determinations

The determination of THg_D was conducted by means of a specific detector (Mercur, Analytik Jena, Jena, Germany) after a pre-reduction of the sample with NH_2OH–HCl (30%, 0.25 mL) followed by a reduction with $SnCl_2$ 2% in HCl 4% using the cold vapour atomic fluorescence spectrometry technique (CV-AFS), in accordance with EPA Method 1631e (US EPA, 2002). Each sample was analysed in triplicate, obtaining a good reproducibility of the results (RSD<5%). Instrument calibration was performed by generating a calibration curve from NIST 3133 certified reference solution at different dilution levels. The limit of detection (LOD) and the limit of quantification (LOQ) calculated on the basis of the standard deviations of ten reagent blanks were 0.69 ng L^{-1} and 2.31 ng L^{-1}, respectively.

The method employed for DGM determination has been extensively described elsewhere (O'Driscoll et al., 2019). Briefly, 1 L water aliquots were gently transferred to a borosilicate bubbler and continuously bubbled for 15 min in a closed loop circuit at a constant flow rate of 10 L min^{-1} under low light conditions, creating an equilibrium between aqueous DGM and Hg^0 in the headspace. This allows for the rapid extraction of DGM from the water (>90% of DGM with sparging time of 5 min; O'Driscoll et al., 2003). The bubbler was connected with a real-time Hg^0 analyser (Lumex RA915M, Lumex Instruments, St. Petersburg, Russia) which was used to maintain the air flow through the bubbler by means of its internal pump and to record Hg^0 concentrations in the air in the headspace. The Lumex analyser is based on the atomic absorption spectrophotometry technique with Zeeman correction for background absorption and high frequency modulated light polarisation (ZAAS-HFM; Sholupov et al., 2004). The instrument allows for the determination of Hg^0 in air in a wide range of concentrations (from 2 to 30,000 ng m^{-3}) with an accuracy of 20%. The instrument is calibrated annually by the parent company and calibration was controlled in the field by a self-checking program measuring Hg^0 in an internal accessory cell containing a known quantity of Hg: the obtained relative deviations were always less than ±6%. A disposable PTFE syringe filter placed before the air intake of the Lumex during analysis was used to prevent the entry of moisture in the instrument. DGM concentrations were obtained through the ratio between the air Hg^0 concentrations at equilibrium and the dimensionless Henry's law constant for Hg (H′) (O'Driscoll et al., 2019). Henry's law constant was calculated in function of the temperature of the water sample according to what reported by Andersson et al. (2008). The system was checked through blanks performed by bubbling MilliQ water, resulting in equilibrium Hg^0 concentrations in air lower than the LOD of the Lumex Instrument (2 ng m^{-3}).

Concentrations of DOC were determined by means of a Total Carbon Analyzer TOC-L (Shimadzu, Japan) using a high-temperature catalytic method (Sugimura and Suzuki, 1988). Instrument calibration was performed using potassium phthalate whereas a quality control was ensured by the analysis of a certified surface seawater reference material (Consensus Reference Material, University of Miami, Florida). The method is characterised by a precision of <3% expressed as %RSD.

2.4. Hg^0 fluxes at the water-air interface

For the assessment of Hg^0 fluxes at the water-air interface, a Plexiglas floating FC coupled with the Lumex analyser was employed following the approach described by Bagnato et al. (2013). Plexiglas was chosen due to its robustness and permeability to all visible and much of UV wavelengths (89% UV-A, 64% UV-B; Wang et al., 2006). Briefly, the chamber is open at the bottom to allow the diffusion of Hg^0 from the confined sea surface and has a square base of 50 × 50 cm and an overall height of 80 cm. For the determination of Hg^0 fluxes, the FC was mounted on a floating board of sintered expanded polystyrene incorporated into an aluminium structure. The FC was manually lowered onto the surface of the water with the lower edges immersed 30 cm in the water in order to avoid the entry of air from outside the chamber by ensuring a tight seal with the surface of the sea (Bagnato et al., 2013). During measurements, the headspace of the chamber was constantly flushed through the Lumex internal pump at its specific constant rate of approximately 10 L min^{-1}. This rate is high enough to avoid an excessive build-up of Hg^0 concentrations in the enclosed air which can suppress the evasion from the water surface (Floreani et al., 2022), and Hg^0 concentrations inside the FC were continuously recorded (1 s interval). After FC deployment, internal Hg^0 concentrations reached a steady-state within approximately 10 min, and FC was removed from the surface of the sea after each sampling. The relatively short sampling time allowed for a reduction in the influence of FC on the microenvironment near the sea surface, as long deployment times can modify ambient conditions near the surface enclosed by the chamber leading to biases in flux estimations (Bagnato et al., 2013; Zhu et al., 2016).

The achieved equilibrium concentrations (C_o), corrected for the initial Hg^0 amount in air entering the chamber (C_i) measured for 5 min with the same recording rate (1 Hz) before placing the chamber on the sea surface, were used for the calculation of fluxes (F) according to Eq. (1) (Bagnato et al., 2013; Kalinchuk et al., 2021):

$$F = \frac{(C_o - C_i)\, Q}{A} \quad (1)$$

where Q is the air flow rate through the chamber (0.6 m^3 h^{-1}) and A is the basal area of the chamber (0.25 m^2). Values of Hg^0 concentration below the Lumex LOD were set to 1 ng m^{-3} (1/2 LOD) according to the

Table 1
Summary of data collected during the sampling campaigns at the selected sites. Data are reported as mean ± SD (min-max); n.a. = not available. Wind data provided as hourly averages by Weather Forecast Regional Observatory of Friuli Venezia Giulia region (OSMER-ARPA FVG) and Slovenian Environmental Agency (ARSO) through database OMNIA (http://www.meteo.fvg.it/). *Values below the instrumental LOQ.

	Val Noghera (VN)			Bay of Piran (PR)		
	Summer (n = 13)	Autumn (n = 14)	Spring (n = 13)	Summer (n = 11)	Autumn (n = 13)	Spring (n = 12)
Air temp. (°C)	25.2 ± 4.2 *(19.7-32.5)*	13.8 ± 5.7 *(8.3-21.9)*	21.4 ± 4.3 *(15.5-27.8)*	21.0 ± 3.7 *(16.0-25.2)*	11.5 ± 3.6 *(7.5-17.3)*	22.1 ± 3.6 *(17.6-28.5)*
UV radiation (W m^{-2})	15.3 ± 18.0 *(0.0-49.3)*	6.4 ± 8.2 *(0.0-19.8)*	20.7 ± 20.5 *(0.0-50.4)*	15.7 ± 16.6 *(0.0-47.7)*	3.8 ± 5.0 *(0.0-12.6)*	16.6 ± 19.8 *(0.0-48.8)*
Wind speed (m s^{-1})	2.6 ± 1.6 *(0.4-5.4)*	1.6 ± 1.0 *(0.1-3.6)*	1.7 ± 1.2 *(0.2-4.0)*	2.3 ± 0.7 *(1.1-3.4)*	3.3 ± 1.1 *(1.5-5.2)*	2.6 ± 1.1 *(0.6-4.2)*
Water temp. (°C)	25.31 ± 0.78 *(24.31-26.55)*	13.16 ± 0.78 *(11.97-14.42)*	23.68 ± 1.44 *(21.35-26.11)*	24.45 ± 0.62 *(23.50-25.80)*	15.38 ± 0.44 *(14.87-16.14)*	22.42 ± 0.47 *(21.93-23.28)*
Salinity (PSU)	38.48 ± 0.23 *(37.85-38.74)*	24.13 ± 0.25 (23.37–24.40)	35.19 ± 0.09 *(34.98-35.32)*	34.73 ± 0.60 *(34.00-35.50)*	35.74 ± 0.22 *(35.26-36.03)*	37.90 ± 0.37 *(37.31-38.51)*
Dissolved O_2 (mg L^{-1})	5.88 ± 1.37 *(4.15-8.32)*	7.97 ± 0.44 *(6.93-8.41)*	6.55 ± 1.35 *(4.01-8.38)*	5.45 ± 0.80 *(5.08-5.90)*	8.52 ± 0.35 *(7.55-8.93)*	6.28 ± 0.36 *(5.72-6.92)*
DOC (mg L^{-1})	10.7 ± 0.7 *(10.1-12.0)*	5.7 ± 0.4 *(5.1-6.5)*	n.a.	n.a.	1.4 ± 0.2 *(1.2-1.9)*	1.8 ± 0.3 *(1.5-2.5)*
THg_D (ng L^{-1})	21.07 ± 4.38 *(15.38-30.95)*	7.26 ± 2.39 *(5.18-14.92)*	12.27 ± 2.99 *(7.69-19.08)*	1.36 ± 0.43* *(0.80*-2.10*)*	2.29 ± 1.34* *(<0.69- 4.31)*	2.00 ± 1.50* *(0.91*-6.45)*
DGM (pg L^{-1})	253.4 ± 45.7 *(176.9-367.3)*	179.1 ± 27.7 *(126.0-224.2)*	430.2 ± 134.0 *(243.5-711.3)*	42.0 ± 12.9 *(28.6-68.7)*	29.7 ± 8.0 *(21.8-52.6)*	107.5 ± 37.1 *(65.5-183.4)*
DGM/TDHg (%)	1.14 ± 0.22 *(0.81-1.59)*	2.61 ± 0.63 *(1.12-3.42)*	3.57 ± 0.93 *(1.66-5.43)*	2.90 ± 1.18 *(0.53-4.89)*	1.91 ± 1.46 *(0.55-6.07)*	6.70 ± 3.19 *(2.35-12.08)*
C_i Hg^0 conc. (ng m^{-3})	4.38 ± 2.71 *(<2-13.59)*	<2 *(<2-6.58)*	2.97 ± 0.66 *(<2-14.35)*	<2 *(<2-5.83)*	2.60 ± 0.72 *(<2-6.72)*	2.15 ± 0.35 *(<2-6.62)*
Hg^0 flux (ng m^{-2} h^{-1})	21.35 ± 6.81 *(9.42-34.38)*	12.25 ± 4.32 *(8.04-24.72)*	23.60 ± 10.85 *(7.43-41.17)*	36.58 ± 25.15 *(2.25-81.49)*	11.32 ± 9.85 *(0.27-38.42)*	18.37 ± 22.01 *(2.38-79.96)*

medium bound approach (United States Environmental Protection Agency Office of Environmental Information, 2000) previously adopted also for other measurements of atmospheric Hg^0 in this area (e.g. Acquavita et al., 2017; Barago et al., 2020).

The QA/QC protocol involved the use of blanks performed in the field by placing the chamber on a clean white polycarbonate surface which showed negligible values and internal Hg^0 concentrations close to the Lumex limit of detection (2 ng m^{-3}). Before and after each sampling campaign the chamber was cleaned with a diluted laboratory detergent and carefully rinsed several times with MilliQ water.

2.5. Statistical analysis

For statistical analysis, *R Software 4.1.3* (R Foundation for Statistical Computing, Vienna, Austria) and the *ggplot2* package (Wickham et al., 2016) were used. The normal distribution of data was assessed using the Shapiro-Wilk test. As sample data were found to be not normally distributed, the non-parametric Kendall rank correlation coefficient was used to evaluate the strength of the associations between variables. Furthermore, the non-parametric Kruskal-Wallis test (K–W) was utilised to assess the occurrence of statistically significant differences between two or more groups of independent variables. If statistically significant differences were found, Dunn's post-hoc test was performed to identify which groups of data differed.

3. Results and discussion

A summary of data collected during the different sampling campaigns at both selected sites is depicted in Table 1. There were optimal weather conditions throughout sampling days, with only an intermittent light cloud cover during morning periods of summer sampling at VN, which did not significantly affect the incident UV radiation recorded during flux measurements, and a short rain event at 2:00 a.m. during summer at PR.

3.1. Total dissolved mercury (THg_D)

Total dissolved Hg concentrations in the surface water at VN were significantly higher ($p < 0.0001$, K–W) than those observed at PR in all seasons. Overall, THg_D concentrations at VN ranged between 5.18 and 30.95 ng L^{-1} (average = 13.38 ± 6.64 ng L^{-1}, n = 40): these values are within the range previously reported for this area (3.39–71.46 ng L^{-1}; Floreani et al., 2019) and below the European Environmental Quality Standard (EQS) for Hg in surface water (70 ng L^{-1}, Directive, 2008/105/CE). The highest THg_D concentrations were recorded in summer and the lowest in autumn (Fig. S1a), likely as a result of diffusive effluxes of Hg species from contaminated sediments into the water column as a function of temperature or release from the degradation of organic matter (Cossa et al., 2009; Covelli et al., 2008; Schartup et al., 2015) as previously observed at this site (Petranich et al., 2018b). These effluxes may have influenced THg_D concentration in the entire water column due to shallow depth (~2 m), resulting in irregular fluctuations of THg_D during sampling periods. Conversely, THg_D concentrations at PR were less variable and significantly lower than those found at VN, being usually <5 ng L^{-1} (average = 1.97 ± 1.24 ng L^{-1}, n = 35), with only one sample exceeding this amount (spring t0: THg_D = 6.45 ng L^{-1}). At this site, no significant differences were observed between values found in the various seasons (Fig. S1b). Moreover, a THg_D concentration of 10.40 ng L^{-1} was detected in summer at t8, which can be considered an outlier ($p < 0.05$, Dixon Q test) and was not used for further elaboration. These concentrations are higher than the average THg_D estimated for the surface water of the Mediterranean Sea (0.17 ± 0.05 ng L^{-1}) (Cossa et al., 2022) and are comparable to the values reported for the Gulf of Trieste (0.12–4.90 ng L^{-1}) (Faganeli et al., 2003), but are generally lower than those observable in the northern part of the Gulf near the mouth of the Isonzo River (0.46–15.4 ng L^{-1}) (Covelli et al., 2006), more affected by the riverine Hg inputs from the area around Idrija (Faganeli et al., 2003).

3.2. Dissolved gaseous mercury (DGM)

The concentrations of DGM at the fish farm site varied between 126.0

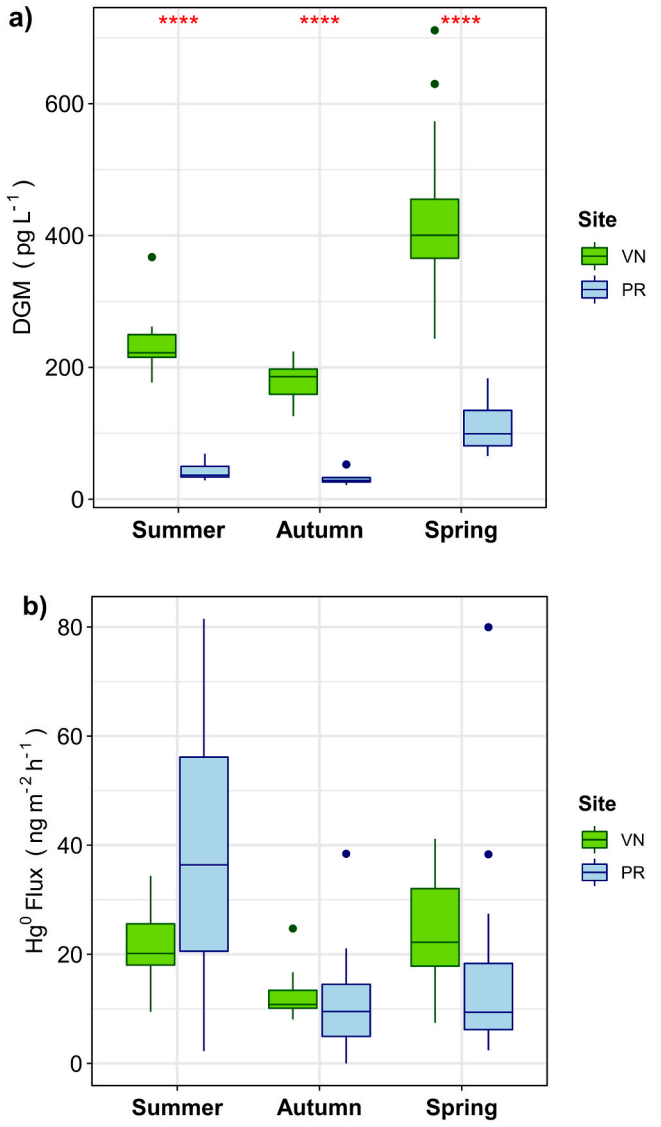

Fig. 2. Distribution of values recorded in the various seasons of (a) DGM concentrations and (b) Hg^0 fluxes in the two selected sampling sites, Val Noghera fish farm (VN) and the Bay of Piran (PR). Red asterisks indicate the statistically significant differences according to Kruskal-Wallis test (****p < 0.0001). (For interpretation of the references to colour in this figure legend, the reader is referred to the Web version of this article.)

and 711.3 pg L^{-1} (average = 278.5 ± 135.1 pg L^{-1}, n = 40) and were comparable to those previously reported for this site (200.3–321.5 pg L^{-1}; O'Driscoll et al., 2019) and for the open Marano and Grado Lagoon (17.3–795.0 pg L^{-1}; Emili et al., 2012). As expected, DGM concentrations encountered at Piran were significantly lower than those obtained at VN in every season ($p < 0.0001$, K–W) and ranged between 21.8 and 183.4 pg L^{-1} (average = 59.4 ± 41.4 pg L^{-1}, n = 36), in good agreement with values previously recorded in another study conducted near our sampling station (33.2–168.0 pg L^{-1}; Kotnik et al., 2022) and within the range reported in the literature for the Gulf of Trieste (40–860 pg L^{-1}; Andersson et al., 2007; Bratkič et al., 2013; Covelli et al., 2006; Kotnik et al., 2015). The higher DGM concentrations found at VN are undoubtedly related to the higher degree of Hg contamination at this site, resulting in higher THg_D concentrations and subsequent greater abundance of Hg forms available for the conversion to DGM. The weak but positive correlation observed between THg_D and DGM concentrations at VN ($\tau = 0.30$, $p < 0.01$, n = 40) may confirm a common source of these two species or that THg_D is the substrate for DGM formation (Marumoto and Imai, 2015), whereas no relationship between these two parameters was detected at PR likely due to the relatively constant THg_D concentrations recorded at this site. However, DGM accounted for only a relatively small portion of THg_D (0.81–5.43% at VN and 0.53–12.08% at PR) in agreement with percentages reported in other studies (Cheng et al., 2019; Conaway et al., 2003; Kotnik et al., 2015; Soerensen et al., 2013; Wang et al., 2020a) and consequently even the relatively low THg_D concentrations recorded at PR did not likely represent a limiting factor for DGM production (Castelle et al., 2009). DGM concentrations found in this work are generally higher than those reported in the literature for other coastal areas subject to lower Hg supplies than the Gulf of Trieste, such as the Tagus Estuary (13.4–40.0 pg L^{-1}; Cesário et al., 2017a), Arcachon Bay (5–193 pg L^{-1}; Bouchet et al., 2011), the Gironde Estuary (2–150 pg L^{-1}; Castelle et al., 2009), and the Thau Lagoon (15.1–63.1 pg L^{-1}; Sharif et al., 2013).

At both sites, significant ($p < 0.05$, K–W) differences were observed between DGM concentrations determined during the various seasons (Fig. S2), with maximum and minimum values recorded during spring and autumn sampling, respectively (Fig. 2a). It must be emphasised that spring measurements were performed late in the season and thus characterised by relatively high values of both UV radiation and water temperature, comparable to those recorded in summer (Table 1), which likely promoted higher DGM production. This hypothesis may be supported by the overall weak positive relationships found between DGM concentrations and incident UV radiation at both sites (VN: $\tau = 0.24$, $p < 0.05$, n = 40; PR: $\tau = 0.40$, $p < 0.001$, n = 36 Fig. S3). Taking into consideration data recorded during daylight hours, slightly better relationships were observed (VN: $\tau = 0.42$, $p < 0.01$, n = 23; PR: $\tau = 0.42$, $p < 0.01$, n = 20) further confirming the role of UV irradiation on DGM production. Many studies observed the occurrence of highest seasonal DGM concentration during period of high insolation and temperatures, promoting both photochemical and biotic reduction (Baeyens and Leermakers, 1998; Ci et al., 2011; Rolfhus and Fitzgerald, 2001; Wang et al., 2016; Wang et al., 2020a). It is widely accepted that photoreduction is a key process in the formation of DGM in surface waters (Ci et al., 2016; Costa and Liss, 1999; Lanzillotta et al., 2002; Soerensen et al., 2013). Various mechanisms have been proposed for the photochemical reduction of Hg^{2+}, including direct photolysis and secondary photochemical processes mediated by photo-produced reducing agents (e.g. oxygen radical species) or by ligand-metal charge transfer in Hg-DOM complexes (Luo et al., 2020).

The interaction between Hg and DOM plays a key role in the activation of photochemical Hg^{2+} reduction, as a relevant fraction of the photoreducible Hg^{2+} present in the water column could be associated with functional groups of DOM in weakly bound complexes (O'Driscoll et al., 2018; Zheng and Hintelmann, 2009): if it is rich in chromophoric groups, DOM can absorb incident radiation and transfer its energy to adsorbed Hg^{2+}, favouring its reduction (Costa and Liss, 1999; Fantozzi et al., 2013, 2007). As a result, an increase in DOM concentration can promote the photo-induced formation of DGM, especially at low THg_D/DOC ratios (Wang et al., 2020b) such as those observed in this study and confirmed by the positive relationships found between DOC and DGM concentrations both at VN and PR (VN: $\tau = 0.44$, $p < 0.01$, n = 27, n = ; PR: $\tau = 0.37$, $p < 0.05$, n = 25, Fig. S3). However, modification of DOM related to photobleaching might reduce this effect over time as a result of a progressive increase in the relative abundance of thiol functional groups and of the proportion of Hg^{2+} strongly bound to these sites, less available to photoreduction (Luo et al., 2020). This may help explain the observed seasonal trend in DGM concentration progressively decreasing from late spring to late autumn particularly at site VN, characterised by higher DOC concentrations in the water (Table 1) likely because of OM degradation, efflux from sediments and the excretion of photosynthetases (Petranich et al., 2018a). This is in agreement with a progressive decrease in Hg^{2+} photoreduction rates due to a progressive DOM photobleaching, as observed in other studies (Amyot et al., 2004;

Costa and Liss, 1999; O'Driscoll et al., 2022). Moreover, the strong mineralisation of organic matter occurring at this site (Petranich et al., 2018a) may also have contributed to enhance the reducible pool of Hg^{2+} in water (Schartup et al., 2015; Živković et al., 2022). The occurrence of strong OM mineralisation in the fish farm (VN) was confirmed by trends of DO_2 concentrations (Fig. 3), characterised by a progressive decrease during the afternoon and night until reaching oxygen depletion ($DO_2 < 5$ mg L^{-1}) in the early morning likely as a result of high oxygen consumption coupled with the low hydrodynamics typical of this site (De Vittor et al., 2012; Petranich et al., 2018a). This diurnal pattern was more evident during summer and spring measurements, whereas in autumn higher and less variable DO_2 concentrations were observed coupled with relatively lower DOC and DGM concentrations.

Considering the PR site, a recent study (Bratkič et al., 2018) found a peak in photochemical reduction during spring in the nearby waters of the Gulf of Trieste, which may explain the high spring DGM concentrations recorded in our work. A second peak in Hg^{2+} reduction was identified in autumn and related to phytoplankton (diatomaceous) bloom and associated bacterial taxa which contain known Hg reducers such as *Rhodobacteraceaea* and *Gammaproteobacteria*; this autumn Hg^{2+} reduction peak may potentially explain the relatively high DGM observed in our study in November, only slightly lower than those found in summer (Fig. S2b). The overall positive relationship found in this study between DGM concentrations and water temperature (Fig. S3) can further support a link between DGM production and biological activity, whose rates are strongly related to temperature (Ahn et al., 2010; Chen et al., 2020). Microorganisms can contribute to DGM formation through both direct Hg^{2+} reduction and the excretion of exudates able to reduce Hg^{2+}, sometimes after light activation (Lanzillotta et al., 2004; Liang et al., 2022; Mason et al., 1995; Wu and Wang, 2014). Even though the relative importance of these two pathways is still poorly understood (Grégoire and Poulain, 2014; Liang et al., 2022), recent findings indicate that biotic mediated Hg^{2+} reduction with or without light account for a relevant fraction of DGM production in water (Kuss et al., 2015). Direct biotic Hg^{2+} reduction can occur even in the absence of light throughout the whole day and water column, consequently representing an important pathway for DGM production in bottom water layers and sediments (Fantozzi et al., 2009; Lepak et al., 2021; Poulain et al., 2004). This process is mainly catalysed by mercury reductase enzyme present in the cytoplasm of Hg-resistant bacteria as a result of the expression of *mer* operon (Barkay et al., 2003). Considering the high Hg concentrations found at VN, the possible presence of Hg-resistant bacteria able to reduce Hg^{2+}, previously documented for the nearby sediments of the Marano and Grado Lagoon (Baldi et al., 2012), could potentially explain the diurnal trend observed for DGM at this site, characterised in all seasons by DGM values during the night which were comparable to those observed during day (Fig. 3, S4a).

The positive relationship between DGM concentration and water temperature found at this site (Fig. S3) may further confirm this hypothesis since temperature represents the primary control on Hg^{2+} dark reduction (Lamborg et al., 2021). However, it cannot be excluded that these relatively high nocturnal DGM concentrations are related to other processes, such as dark abiotic reduction mediated by organic matter (e.g. humic substances) or demethylation. Humic substances can directly reduce Hg^{2+} in the absence of light thanks to the interaction with reducing intermediates such as quinones (Allard and Arsenie, 1991; O'Driscoll et al., 2004; Vudamala et al., 2017), and this effect may have been favoured by the relative high DOC concentration observed at VN (Table 1). Moreover, previous studies have indicated that both reductive and possibly oxidative demethylation could occur in the sediments of the studied area and of the whole Gulf of Trieste (Hines et al., 2017; Petranich et al., 2018b) producing either Hg^0 or Hg^{2+} available for reduction. In environments characterised by high Hg levels, biotic reductive demethylation is generally favoured due to the presence of various Hg resistant bacteria with the *mer* system. The formation and subsequent volatilisation of Hg^0 indeed represent an important detoxification pathway for these microorganisms (Barkay and Gu, 2022). Finally, effluxes from anoxic sediments due to the dissolution of Hg adsorbent compounds such as iron or manganese hydroxides are also possible (Bouffard and Amyot, 2009), considering the shallow depth (~2 m) of the water column at this site. Sediment benthic fluxes may have influenced also the amount of Hg^{2+} in the water column available for reduction as Hg can be released from sediments both in Hg^{2+} or Hg^0 form (Acquavita et al., 2021). However, it should be noted that during the day DGM concentrations at VN roughly followed the pattern of UV radiation with a slight delay, confirming the previous observations made at this site (O'Driscoll et al., 2019) and indicating that under light conditions, the formation of DGM in the water column may be largely related to photo-induced processes. A better agreement between UV radiation and DGM variation was observed at the Bay of Piran (PR), with peak DGM concentrations observed in the central part of the day in all seasons and lower and relatively constant concentrations during the night (Fig. 4, S4b), with minimum values recorded between 4 and 6 am.

These results further confirm the relevance of photochemical processes at this site.

3.3. Hg^0 fluxes at the water-air interface

The Hg^0 fluxes recorded at the Val Noghera (VN) fish farm during this study varied between 7.43 and 41.17 ng m^{-2} h^{-1}, with an overall average of 18.90 ± 9.05 ng m^{-2} h^{-1} (n = 40), whereas at Piran (PR) Hg^0 emission showed a greater variability, ranging between 0.27 and 81.49 ng m^{-2} h^{-1} with an overall average of 21.39 ± 21.90 ng m^{-2} h^{-1} (n = 36). Considering the significantly higher DGM concentrations observed at VN than at PR, the comparable and in some cases slightly higher fluxes calculated for this latter site were unexpected. This discrepancy may be explained by the different hydrodynamism of the selected sites. The PR site was located in an open coastal area subject to marked water turbulence due to waves and tides which could have favoured the release of Hg^0 at the water-air interface extending the surface boundary layer (Ferrara et al., 2000; Zappa et al., 2003). This enhancement is effective mostly when surface water is super-saturated in DGM with respect to the atmosphere (Castelle et al., 2009) which is likely what occurred in this study taking into consideration both the atmospheric Hg^0 levels recorded in ambient air before the chamber deployment (Ci) and the measured DGM concentrations. Overall, atmospheric Hg^0 concentrations (Table 1) were comparable to those previously reported for the Northern Adriatic Sea coastal area (2.70 ± 1.50 ng m^{-3}, Barago et al., 2020) and on average slightly higher than the estimated natural background for the Northern Hemisphere (1.5–1.7 ng m^{-3}, Sprovieri et al., 2010). This may be related to diffuse Hg^0 emissions from the contaminated substrates of this highly impacted area (Floreani et al., 2020). Therefore, DGM concentrations recorded in water were higher than those expected with these atmospheric Hg^0 concentrations according to Henry's law (Andersson et al., 2008), indicating a constant super-saturation in DGM of surface water. Under these circumstances, gaseous exchanges can be more regulated by turbulent mixing conditions rather than the concentration gradient between the water and air (Lindberg and Meyers, 1995; Poissant et al., 2000). Moreover, spikes of high Hg^0 emission at PR (81.49 ng m^{-2} h^{-1} at 6:30 p.m. in summer and 79.96 ng m^{-2} h^{-1} at 7:00 p.m. in spring) were recorded in parallel with increased wave motion observed in the field despite the low irradiation with the subsequent lower photo-production of DGM and the alteration of micro-environmental conditions caused by placing the FC, which should diminish the influence of turbulence (Bagnato et al., 2013). Conversely, VN site in the confined environment of the fish farm was characterised by extremely scarce water movement and the occurrence of stable surface layer conditions may have strongly limited Hg^0 emissions (Osterwalder et al., 2021). The calculated fluxes are in good agreement with the estimated Hg^0 emission rate for the Northern Adriatic Sea (28.4 ± 4.7 ng m^{-2} h^{-1}; Andersson et al., 2007) and by far exceed the estimated annual atmospheric depositions of Hg in this area

Table 2
Comparison of Hg^0 fluxes obtained in this study and over various other coastal and open sea environments. n.a. = not available, FC = flux chamber, MM = micro-meteorological model.

Site	Hg^0 flux (ng m^{-2} h^{-1})		Method	Reference
	av ± std	Min-Max		
Coastal sites				
Val Noghera	18.90 ± 9.05	7.43–41.17	FC	This study
Piran Bay	21.39 ± 21.90	0–81.49	FC	This study
Val Noghera	35.6 ± 12.6	16.4–64.0	FC	Floreani et al. (2019)
Piran Bay	32.2 ± 16.6	6.0–68.0	FC	Floreani et al. (2019)
Gulf of Trieste	5.13 ± n.a.	n.a.	MM	Kotnik et al. (2022)
N Adriatic Sea	28.4 ± 4.7	23.7–33.2	MM	Andersson et al. (2007)
Augusta Bay	23.1 ± 24	3.2–72.1	FC	Bagnato et al. (2013)
Tyrrhenian Sea (near CAP)	n.a.	8.2–44	FC	Ferrara and Mazzolai (1998)
Sardinia coast	3.61 ± 0.98	2.36–4.75	FC	Gårdfeldt et al. (2003)
Arcachon Bay	4.3 ± n.a.	0.4–14.5	MM	Bouchet et al. (2011)
Minamata Bay	5.4 ± 6.3	0.1–33	MM	Marumoto and Imai (2015)
Tokyo Bay	5.8 ± 5.0	0.1–22.1	MM	Narukawa et al. (2006)
Jiaozhou bay	0.67 ± n.a.	−0.15–2.21	FC	Xu et al. (2012)
Bohai Sea	0.8 ± 1.5	−6.1–12.8	MM	Wang et al. (2020a)
Swedish coastal area	0.61 ± n.a.	−0.61–8.8	FC	Gårdfeldt et al. (2001)
Long Island Sound	0.7 ± 0.5	0.1–10.3	MM	Rolfhus and Fitzgerald (2001)
San Francisco Bay	n.a.	2.5–46.0	MM	Conaway et al. (2003)
Offshore marginal seas				
Western Mediterranean Sea	4.5 ± 5.1	−5.6–33.8	MM	Nerentorp Mastromonaco et al. (2017)
Eastern Mediterranean Sea	2.2 ± 1.5	0.2–4.9	MM	Fantozzi et al. (2013)
Baltic Sea	1.3 ± 1.6	−0.13–1.87	MM	Kuss et al. (2018)
North Sea	6.2 ± 5.3	0.5–19.9	MM	Baeyens and Leermakers (1998)
South China Sea	4.5 ± 3.4	0.2–15.3	MM	Fu et al. (2010)
East China Sea	4.1 ± 3.2	0.2–14.8	MM	Wang et al. (2016)
Yellow Sea	18.3 ± 11.8	3.2–44.0	MM	Ci et al. (2011)
Western Pacific marginal seas	1.7 ± 0.6	0.6–2.5	FC	Kalinchuk (2023)
Eastern Arctic Seas	0.67 ± 0.13	0.28–1.35	FC	Kalinchuk et al. (2021)
Open ocean				
Arctic Ocean	0.65 ± 0.19	0.33–0.82	FC	Kalinchuk et al. (2021)
Atlantic Ocean	n.a.	2.1–6.8	MM	Soerensen et al. (2013)
Eastern North Atlantic Ocean	0.6 ± 0.7	n.a.	MM	Mason et al. (2017)
Western North Atlantic Ocean	1.2 ± 1.6	n.a.	MM	Mason et al. (2017)
Pacific Ocean	n.a.	0.7–8.7	MM	Soerensen et al. (2014)
South Pacific Ocean	0.7 ± 0.6	n.a.	MM	Mason et al. (2017)

(1.98–3.25 ng m^{-2} h^{-1}; Tomažič et al., 2018) or in nearby inland area of Iskrba (SLO) (wet deposition = 0.34–1.14 ng m^{-2} h^{-1}; Sprovieri et al., 2017), confirming that these environments may represent a source of Hg for nearby coastal environments under favourable wind conditions (Barago et al., 2020; Wängberg et al., 2008). For example, Hg concentrations detected in lichens collected over the entire Marano and Grado Lagoon (Floreani et al., 2020) roughly followed the same spatial pattern of Hg contamination in sediments, further confirming that Hg^0 evasion from the substrate can heavily impact the atmospheric level of this metal over our study area. Generally, Hg^0 fluxes recorded in our study were comparable to those estimated for other coastal environments and marginal seas surrounded by notable anthropogenic sources of Hg (e.g. Augusta Bay, Italy; San Francisco Bay, USA; Minamata Bay, Japan; Yellow Sea, China; Table 2), highlighting the importance of the discharges of this metal from past human activities in promoting the occurrence of high DGM concentrations in surface water and its subsequent release into the atmosphere. Moreover, fluxes calculated in this study are higher than those commonly reported for offshore areas (Table 2), where Hg amounts involved in exchanges between environmental compartments are generally lower than coastal areas due to lower supplies of this metal from river transport and/or direct anthropogenic discharges (Amos et al., 2014; Fitzgerald et al., 2007; Marumoto and Imai, 2015). However, it must be stressed that comparison among Hg^0fluxes reported in different studies should be interpreted with great caution as a standard protocol for measurements does not yet exist (Sommar et al., 2020; Zhu et al., 2016). Hg^0 fluxes at the water-air interface can be directly evaluated through the use of FCs or computed through several gas-exchange models. In the first case, differences in size, shape, and turnover time of air inside the chamber could significantly affect the calculated flux value (Eckley et al., 2010; Zhu et al., 2015) whereas the choice of gas-exchange model could lead to different Hg^0 flux estimations due to different parametrisation of Hg transfer velocities from water (Nerentorp Mastromonaco et al., 2017; Osterwalder et al., 2021; Sharif et al., 2013). The same experimental approach used in the present study was previously adopted in a preliminary investigation of Hg^0 fluxes at the water-air interface in different coastal areas of the northern Adriatic Sea (Floreani et al., 2019). Two of the sites investigated in the cited study correspond to those selected in this work and generally showed higher emissions likely due to the fact that measurements were performed only during the diurnal period when a greater DGM formation is expected, as partially confirmed by our results. Even though DGM was not measured in the cited study, the higher THg_D concentrations recorded in particular at VN also suggest a greater abundance of substrate available for the reduction of Hg^{2+} to DGM and its subsequent release to the atmosphere. Moreover, our results are comparable to fluxes previously measured with the same experimental approach in freshwater environments upstream from our study area, the Solkan Reservoir along the Isonzo River (21.88 ± 11.55 ng m^{-2} h^{-1}) and the dockyard of the Torviscosa chlor-alkali plant (19.01 ± 12.65 ng m^{-2} h^{-1}) (Floreani et al., 2022), impacted by the same contamination sources responsible for Hg inputs into the Gulf of Trieste and the Marano and Grado Lagoon.

Considering the seasonal variation, at both sites the lowest Hg^0 fluxes were found in autumn: values calculated in this season were significantly ($p < 0.05$, K–W) lower than those observed in summer and spring at the fish farm (VN), whereas at PR only Hg^0 fluxes recorded in summer were significantly different from those of autumn (Fig. 2b, S5). At VN, the seasonal pattern of Hg^0 fluxes characterised by highest values in spring is in agreement with that of DGM concentrations (Fig. 2). The positive relationship observed between DGM concentration and Hg^0

fluxes at this site ($\tau = 0.43$, $p < 0.001$, $n = 40$, Fig. 5) further confirms the importance of the availability of the volatile Hg^0 to support relevant emissions into the atmosphere (Baeyens and Leermakers, 1998; Kalinchuk et al., 2021; Osterwalder et al., 2021). However, Hg^0 fluxes calculated for the spring were comparable to those observed in summer (Fig. S5a) despite the significantly lower DGM concentrations found in this last period (Fig. S2a). A potential explanation for this trend lies in the lower water temperatures recorded during spring compared to summer, which may have limited gaseous evasion due to lower diffusivity and the higher solubility of DGM under these conditions (Andersson et al., 2008; Kuss et al., 2009; Sanemasa, 1975). Indeed, an overall positive relationship between fluxes and water temperature at VN ($\tau = 0.39$, $p < 0.001$, $n = 40$, Fig. S6) was observed, confirming that this parameter plays a key role in controlling the magnitude of Hg^0 evasion into the atmosphere, as observed in numerous studies (Bouchet et al., 2011; Chen et al., 2020; Kalinchuk, 2023; Kalinchuk et al., 2021; Poissant et al., 2000; Soerensen et al., 2013; Wang et al., 2020a). An overall weak positive relationship between Hg^0 fluxes and surface water temperatures was also found at PR ($\tau = 0.29$, $p < 0.01$, $n = 36$). In this case, as also seen at VN, higher water temperatures in summer could help explain the different seasonal variation between DGM concentration and Hg^0 fluxes. Indeed, the lowest average emission was observed in autumn and the highest in summer despite DGM concentrations lower than those observed in spring (Fig. 2), even though, as stated above, fluxes at this site may have been deeply influenced by water turbulence.

At the fish farm, Hg^0 fluxes could also have been limited by the competition of the evasion process with the re-oxidation of DGM to non-volatile Hg^{2+}, which can occur at the same time as the reduction under sunlight, mainly due to photochemical reactions leading to the production of oxidants such as single oxygen or hydroxyl or carbonate radicals (Garcia et al., 2005; He et al., 2014; Luo et al., 2020). Moreover, oxidation rates can be significantly enhanced with increasing salinity, even in the absence of light (Ci et al., 2016; Lalonde et al., 2001) thanks to the presence of halides (e.g. Cl^-, Br^-) which can react with hydroxyl radical to form additional oxidants (Whalin et al., 2007) or stabilise Hg oxidation products through the formation of non-photoreducible complexes (Qureshi et al., 2010; Yamamoto, 1996). Previous studies have indicated that losses of DGM through photo-oxidation in saltwater can be dominant compared to volatilisation (Ci et al., 2016; Lalonde et al., 2004). An increase in DGM oxidation rates and decrease in volatilisation can increase the amount of Hg retained in the water column, mostly in static water environments such as the fish farm (VN), whereas in more dynamic conditions, such as those encountered at PR, most of the produced DGM can be readily lost to the atmosphere (Clarke et al., 2023; Zhang et al., 2021). In addition, considering the high DOC concentrations observed in this site, a potential contribution of direct adsorption of DGM on functional groups of OM in reducing the amounts available for volatilisation cannot be ruled out, as previous studies indicate that a relevant fraction of elemental Hg can occur in this phase in natural waters (Wang et al., 2015). Finally, during spring sampling at VN, a notable macrophyte bloom was observed in the field, coupled with the formation of a transparent biological film on the surface of the water, which may have further limited the diffusion of Hg^0 into the atmosphere (Osterwalder et al., 2021). All these aspects could lead to a longer residence time of Hg in the water column. A rough estimation based on daily averages of THg_D and Hg^0 fluxes recorded in the different seasons at the fish farm indicate that the Hg lost through volatilisation represents only a small percentage of the total amount of this metal occurring in the dissolved phase in surface water. Particularly in summer, losses through volatilisation accounted for only 2.4% of THg_D per day, whereas slightly higher relative contributions were observed in autumn (4.0%) and spring (4.6%). Conversely, at the more dynamic environment of Piran, emissions of Hg^0 were more effective, then causing, on daily basis, an estimated loss through volatilisation equal to 11.9% of THg_D in autumn, 22.0% in spring and 64.6% in summer.

As a result, the relatively low amounts of losses through volatilisation at the fish farm can potentially lead to a greater Hg availability for methylation after oxidation to Hg^{2+}, which can occur even in microenvironments in oxic water layers such as periphyton, roots of macrophytes, and settling particles, and in a favoured incorporation into the trophic web (Branfireun et al., 2020; Colombo et al., 2013; Jung et al., 2022; Zhang et al., 2021). This aspect may be a great concern in this environment due to the frequent occurrence of environmental conditions favourable for Hg methylation such as reduced DO_2 levels related to strong OM mineralisation (Petranich et al., 2018b), particularly in summer when the lowest relative loss of Hg through volatilisation has been observed. Relatively high methylation rates, comparable with those observed in anoxic sediments, can indeed occur even in the water column, mostly at depths of maximum oxigen consumption (Cossa et al., 2009; Eckley and Hintelmann, 2006; Millard et al., 2023), but have also been observed in surface waters of a Mediterranean coastal lagoon (Monperrus et al., 2007). Furthermore, current warming of the climate can further increase the amount of Hg entering the trophic web by lengthening the growing period of phytoplankton and thereby extending its exposure to MeHg (Bełdowska and Kobos, 2016). Moreover, Hg^0 may also be directly subject to biotic or abiotic methylation (Gonzalez-Raymat et al., 2017; Yin et al., 2014) mostly in the presence of halogens and under conditions of strong solar irradiation (Castro et al., 2011) like those which occurred in this study in summer and spring, coupled with a relatively low volatilisation. However, it is still unclear if these reactions occur under environmental conditions (Gonzalez-Raymat et al., 2017). All these aspects may represent a concern for the health of aquatic ecosystem and should be further investigated in future e.g. coupling Hg^0 flux and MeHg concentration measurements at the fish farm under different hydrodynamic conditions, also taking into consideration potential demethylation processes favoured by incident radiation (Klapstein and O'Driscoll, 2018). Photodemethylation can indeed be a significant pathway for MeHg removal in surface water layers where radiation can penetrate, but it is not yet clear whether this degradation leads to the production of Hg^0 or Hg^{2+} and thus the influence of this process on gaseous exchanges of Hg is still unclear (Barkay and Gu, 2022; Seller et al., 1996).

Considering the diurnal variability of Hg^0 fluxes (Figs. 3–4), positive values were calculated for all measurements at both sites , with nighttime fluxes generally slightly lower than those observed during the day (Fig. 6). This indicates a constant supply of DGM in the surface waters supported by the efficient above-described DGM production or transport processes even in the absence of light. This applies especially to the fish farm site (VN), whereas at PR slightly higher differences between day and night Hg^0 fluxes were generally observed likely confirming a greater importance of photochemical processes as already observed for DGM. Interestingly, the peak Hg^0 fluxes at VN were always recorded at sunset, corresponding to the inversion of the temperature gradient between the air and water, which may have influenced the transfer velocity of DGM between these two compartments (Poissant et al., 2000; Vette et al., 2002). Generally, at both sites, fluxes gradually decreased during the night, reaching the minimum before sunrise followed by a relatively sharp increase in the morning, roughly following a temporal pattern similar to that observed for DGM concentrations. This confirm that factors influencing DGM formation also impact gaseous evasion at the water-air interface (Cesário et al., 2017b). However, some differences between temporal patterns of DGM and fluxes were observed: fluxes at VN generally showed a decrease from late morning to afternoon coupled with increasing DGM concentration, whereas at PR, the progressive reduction of fluxes during the night was accompanied by relatively constant DGM values. These findings suggest that evasion is more regulated by physical parameters influencing air-sea gaseous exchanges rather than DGM concentrations alone (Lindberg and Zhang, 2000), as confirmed by the weak relationship between these two parameters at PR (Fig. 5).

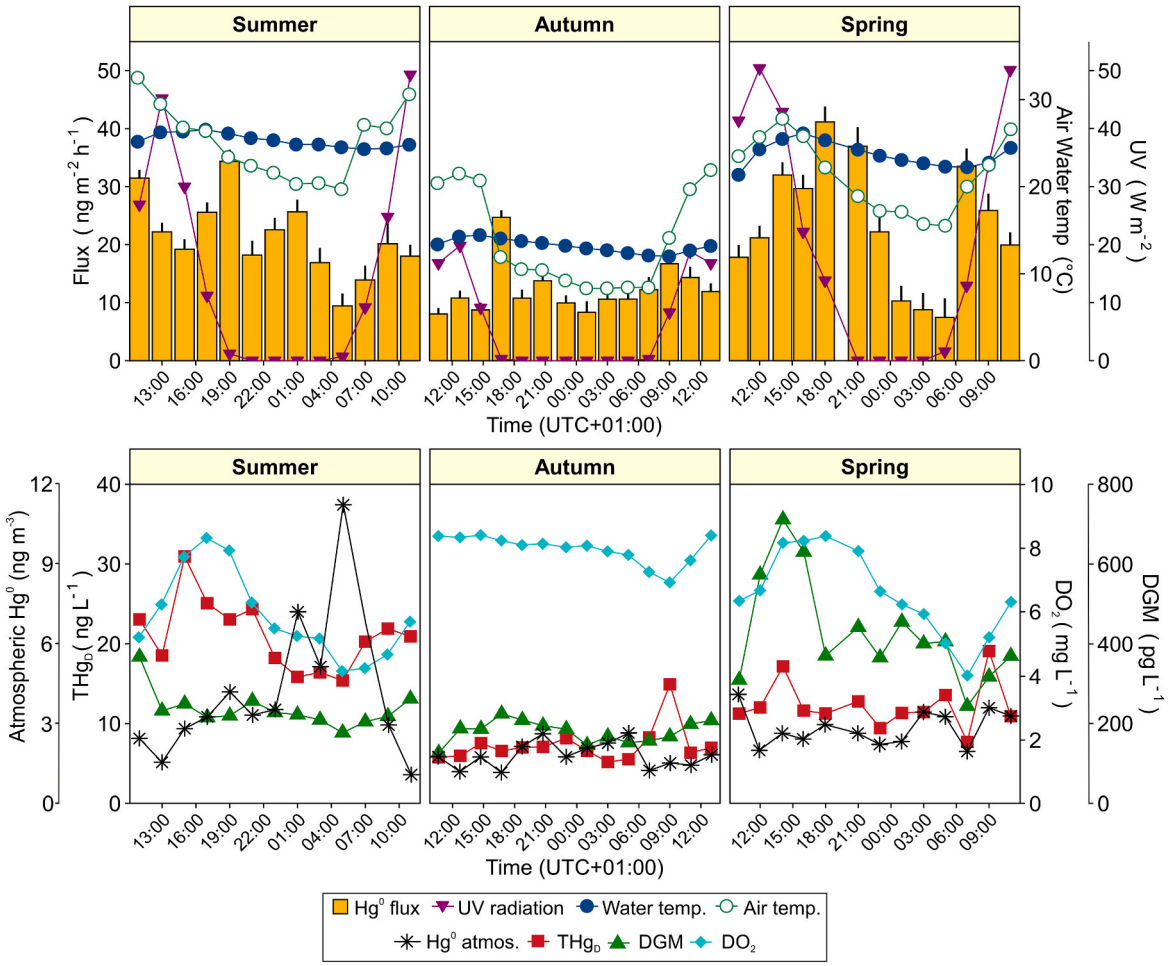

Fig. 3. Diurnal patterns of Hg^0 fluxes, UV radiation, water and air temperatures, initial atmospheric Hg^0 (Ci), THg_D, DGM, and dissolved oxygen (DO_2) concentrations in the different seasons at Val Noghera fish farm (VN).

4. Conclusions

A significant production of DGM was observed in this study at the Val Noghera (VN) fish farm as a result of the combination of photoreduction of Hg^{2+} during the day and abiotic and biotic reduction reactions during night and day, which can occur both in shallow water and in contaminated sediments. The comparable DGM concentrations observed during night and day may confirm the importance of processes leading to DGM production in the absence of radiation at this site. Moreover, strong mineralisation of abundant OM present at this site could have further contributed to increase the amount of Hg^{2+} available for reduction reactions. Lower THg_D and DGM concentrations were observed at PR, confirming the lower degree of Hg contamination of this part of the Gulf of Trieste. The highest average DGM concentrations at both sites were observed during spring and the lowest in autumn following the same temporal pattern of UV radiation. This suggests that, despite the relevant contribution of dark reduction processes (especially at VN), photoreduction still represented the dominant DGM production pathway.

Relatively high Hg^0 fluxes were recorded at both sites, significantly exceeding the estimated atmospheric Hg deposition rates for this contaminated area, which can therefore be considered as a secondary source of Hg into the atmosphere. Generally, higher Hg^0 fluxes were observed in summer likely due to higher water temperatures which decrease DGM solubility. Moreover, positive fluxes were observed in all sampling periods, thus suggesting a continuous supply of DGM high enough to replace DGM lost through volatilisation even during the night. However, despite the significantly higher DGM concentrations observed at the fish farm, Hg^0 fluxes were comparable to those calculated for the Bay of Piran. This unexpected result may be explained by the different hydrodynamism of the water column at the selected sites: the high water turbulence observed at PR likely promoted a higher rate of Hg^0 emission, whereas water stagnation at VN may have strongly limited gaseous exchanges at this site together with expected high Hg oxidation rates in static lagoon environments, likely favouring the higher retention of Hg in the water column. These results suggest that enhancing water turbulence in confined coastal marine environments could represent a simple mitigation action to increase the amount of Hg lost by the system through volatilisation and to prevent the re-oxidation of DGM to Hg^{2+}, thereby reducing the burden of this ionic form in the aquatic environment available for methylation and incorporation into food webs. Therefore, Hg^0 fluxes should be accurately monitored in this kind of environment which is particularly vulnerable to Hg contamination, as understanding the entity and dynamics of this phenomenon under various conditions could be helpful to assess the ability of these ecosystems to recover from historical and/or contemporary supplies of this metal related to anthropogenic activities.

Credit author statement

Federico Floreani: Conceptualization, Methodology, Investigation, Data curation, Formal analysis, Writing – Original Draft, Writing – Review & Editing, Visualization. **Nicolò Barago:** Investigation. **Katja Klun:** Investigation, Resources. **Jadran Faganeli:** Conceptualization, Validation, Writing – Original Draft, Writing – Review & Editing.

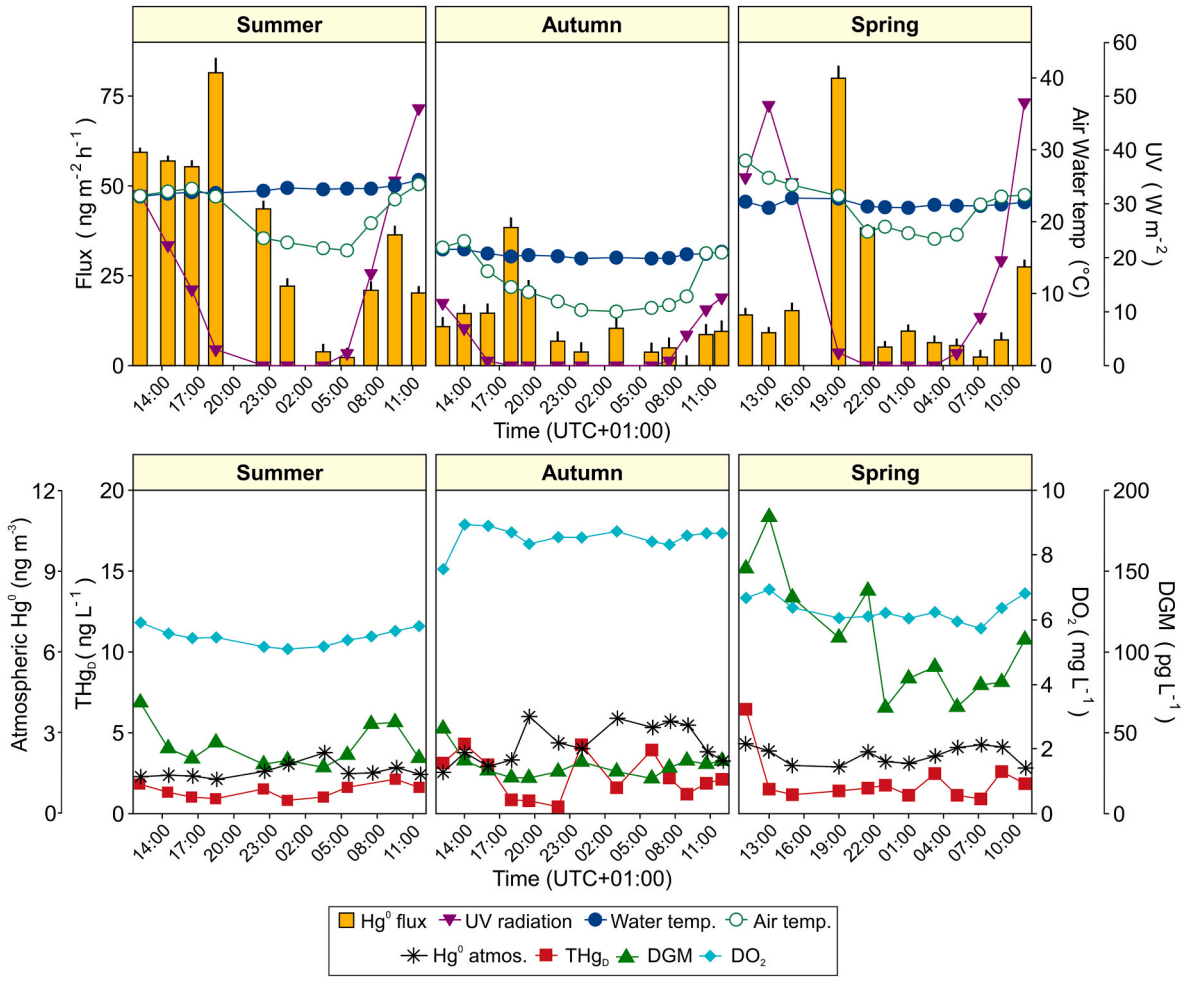

Fig. 4. Diurnal patterns of Hg^0 fluxes, UV radiation, water and air temperatures, initial atmospheric Hg^0 (Ci), THg_D, DGM, and dissolved oxygen (DO_2) concentrations in the different seasons at the Bay of Piran (PR). Note differences in scale on the y-axis compared to the VN sampling station in Fig. 3.

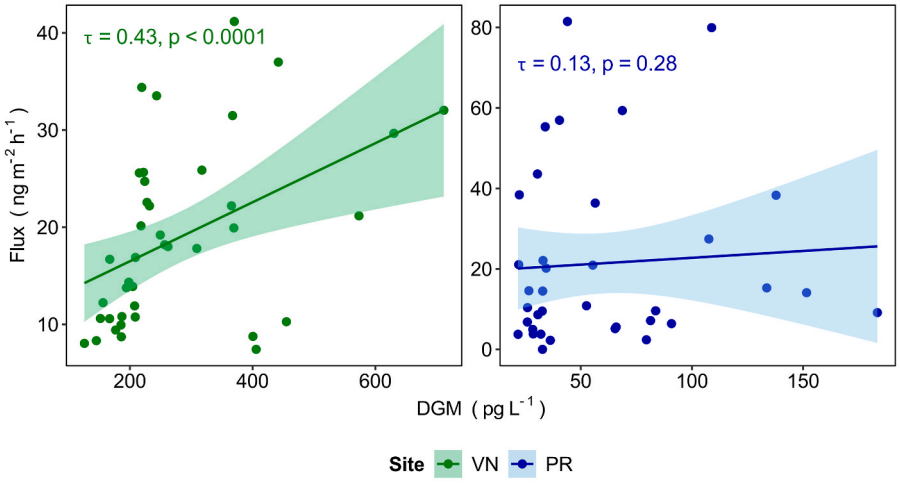

Fig. 5. Overall correlation between DGM concentrations and Hg^0 fluxes at the selected sampling sites, Val Noghera fish farm (VN) and the Bay of Piran (PR). Kendall's rank correlation coefficient (τ) and 95% confidence intervals are reported.

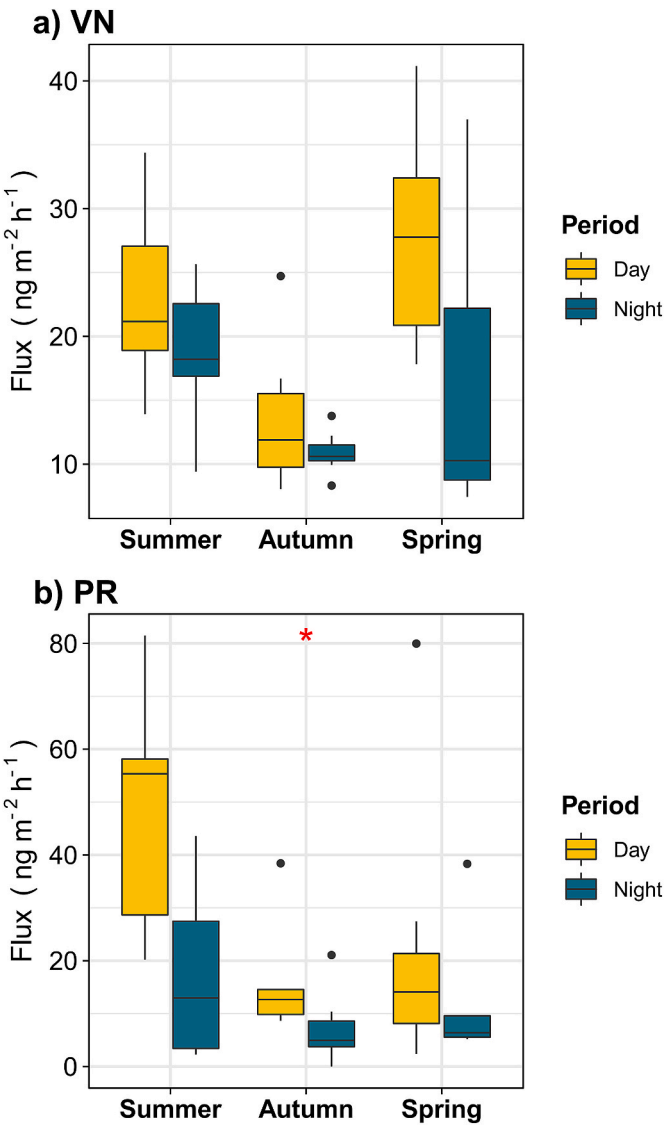

Fig. 6. Distribution of Hg^0 fluxes recorded during day and night at the two sites, Val Noghera fish farm (VN) and the Bay of Piran (PR). Note the difference in Y-axis scale.

Stefano Covelli: Conceptualization, Methodology, Resources, Validation, Writing – Original Draft, Writing – Review & Editing, Project administration, Supervision.

Declaration of competing interest

The authors declare that they have no known competing financial interests or personal relationships that could have appeared to influence the work reported in this paper.

Data availability

Data will be made available on request.

Acknowledgements

This work is part of the Ph.D. thesis written by Federico Floreani at the University of Trieste, Italy; the Ph.D. fellowship was funded by PO FRIULI VENEZIA GIULIA-FONDO SOCIALE EUROPEO 2014/2020. The authors are very grateful to Alessandro Acquavita for his valuable technical assistance during sampling operations and his useful suggestions. A special thanks to Claudio Furlanut, Marco Cambi and the entire staff at Val Noghera Fish Farm for their fundamental logistical support and kind hospitality at the fish farm during field work. Thanks also to Elisa Petranich and to students Gabriele Faoro and Federico Vito Zotta for their support in sampling operations. OSMER-ARPA FVG and ARSO are acknowledged for providing the meteorological wind data. Three anonymous reviewers are acknowledged for the useful suggestions which improved the early version of the manuscript. We warmly thank Karry Close for proofreading the manuscript.

Appendix A. Supplementary data

Supplementary data to this article can be found online at https://doi.org/10.1016/j.envpol.2023.121926.

References

Acquavita, A., Aleffi, I.F., Benci, C., Bettoso, N., Crevatin, E., Milani, L., Tamberlich, F., Toniatti, L., Barbieri, P., Licen, S., Mattassi, G., 2015. Annual characterization of the nutrients and trophic state in a Mediterranean coastal lagoon: the Marano and Grado Lagoon (northern Adriatic Sea). Reg. Stud. Mar. Sci. 2, 132–144. https://doi.org/10.1016/j.rsma.2015.08.017.

Acquavita, A., Biasiol, S., Lizzi, D., Mattassi, G., Pasquon, M., Skert, N., Marchiol, L., 2017. Gaseous elemental mercury level and distribution in a heavily contaminated site: the ex-chlor alkali plant in Torviscosa (Northern Italy). Water, Air. Soil Pollut 228, 62. https://doi.org/10.1007/s11270-016-3234-z.

Acquavita, A., Covelli, S., Emili, A., Berto, D., Faganeli, J., Giani, M., Horvat, M., Koron, N.Ž., Rampazzo, F., 2012. Mercury in the sediments of the Marano and Grado lagoon (northern Adriatic Sea): sources, distribution and speciation. Estuar. Coast Shelf Sci. 113, 20–31. https://doi.org/10.1016/j.ecss.2012.02.012.

Acquavita, A., Floreani, F., Covelli, S., 2021. Occurrence and speciation of arsenic and mercury in alluvial and coastal sediments. Curr. Opin. Environ. Sci. Heal. 22, 100272 https://doi.org/10.1016/j.coesh.2021.100272.

Ahn, M.C., Kim, B., Holsen, T.M., Yi, S.M., Han, Y.J., 2010. Factors influencing concentrations of dissolved gaseous mercury (DGM) and total mercury (TM) in an artificial reservoir. Environ. Pollut. 158, 347–355. https://doi.org/10.1016/j.envpol.2009.08.036.

Allard, B., Arsenie, I., 1991. Abiotic reduction of mercury by humic substances in aquatic system - an important process for the mercury cycle. Water, Air, Soil Pollut. 56, 457–464. https://doi.org/10.1007/BF00342291.

Amos, H.M., Jacob, D.J., Kocman, D., Horowitz, H.M., Zhang, Y., Dutkiewicz, S., Horvat, M., Corbitt, E.S., Krabbenhoft, D.P., Sunderland, E.M., 2014. Global biogeochemical implications of mercury discharges from rivers and sediment burial. Environ. Sci. Technol. 48, 9514–9522. https://doi.org/10.1021/es502134t.

Amyot, M., Gill, G.A., Morel, F.M.M., 1997. Production and loss of dissolved gaseous mercury in coastal seawater. Environ. Sci. Technol. 31, 3606–3611. https://doi.org/10.1021/es9703685.

Amyot, M., Southworth, G., Lindberg, S.E., Hintelmann, H., Lalonde, J.D., Ogrinc, N., Poulain, A.J., Sandilands, K.A., 2004. Formation and evasion of dissolved gaseous mercury in large enclosures amended with 200HgCl2. Atmos. Environ. 38, 4279–4289. https://doi.org/10.1016/j.atmosenv.2004.05.002.

Andersson, M.E., Gårdfeldt, K., Wängberg, I., Sprovieri, F., Pirrone, N., Lindqvist, O., 2007. Seasonal and daily variation of mercury evasion at coastal and off shore sites from the Mediterranean Sea. Mar. Chem. 104, 214–226. https://doi.org/10.1016/j.marchem.2006.11.003.

Andersson, M.E., Gårdfeldt, K., Wängberg, I., Strömberg, D., 2008. Determination of Henry's law constant for elemental mercury. Chemosphere 73, 587–592. https://doi.org/10.1016/j.chemosphere.2008.05.067.

Ariya, P.A., Amyot, M., Dastoor, A., Deeds, D., Feinberg, A., Kos, G., Poulain, A., Ryjkov, A., Semeniuk, K., Subir, M., Toyota, K., 2015. Mercury physicochemical and biogeochemical transformation in the atmosphere and at atmospheric interfaces: a review and future directions. Chem. Rev. 115, 3760–3802. https://doi.org/10.1021/cr500667e.

ARPAFVG-OSMER, 2014. Il clima del Friuli Venezia Giulia (in italian). 27 pp.

Baeyens, W., Leermakers, M., 1998. Elemental mercury concentrations and formation rates in the Scheldt estuary and the North Sea. Mar. Chem. 60, 257–266. https://doi.org/10.1016/S0304-4203(97)00102-3.

Bagnato, E., Sproveri, M., Barra, M., Bitetto, M., Bonsignore, M., Calabrese, S., Di Stefano, V., Oliveri, E., Parello, F., Mazzola, S., 2013. The sea-air exchange of mercury (Hg) in the marine boundary layer of the Augusta basin (southern Italy): concentrations and evasion flux. Chemosphere 93, 2024–2032. https://doi.org/10.1016/j.chemosphere.2013.07.025.

Baldi, F., Gallo, M., Marchetto, D., Fani, R., Maida, I., Horvat, M., Fajon, V., Zizek, S., Hines, M., 2012. Seasonal mercury transformation and surficial sediment detoxification by bacteria of Marano and Grado lagoons. Estuar. Coast Shelf Sci. 113, 105–115. https://doi.org/10.1016/j.ecss.2012.02.008.

Baptista-Salazar, C., Richard, J.H., Horf, M., Rejc, M., Gosar, M., Biester, H., 2017. Grain-size dependence of mercury speciation in river suspended matter, sediments and soils in a mercury mining area at varying hydrological conditions. Appl. Geochem. 81, 132–142. https://doi.org/10.1016/j.apgeochem.2017.04.006.

Barago, N., Floreani, F., Acquavita, A., Esbrí, J.M., Covelli, S., Higueras, P., 2020. Spatial and temporal trends of gaseous elemental mercury over a highly impacted coastal environment (Northern Adriatic, Italy). Atmosphere 11, 935. https://doi.org/10.3390/atmos11090935.

Barkay, T., Gu, B., 2022. Demethylation—The other side of the mercury methylation coin: a critical review. ACS Environ. Au 2, 77–97. https://doi.org/10.1021/acsenvironau.1c00022.

Barkay, T., Miller, S.M., Summers, A.O., 2003. Bacterial mercury resistance from atoms to ecosystems. FEMS Microbiol. Rev. 27, 355–384. https://doi.org/10.1016/S0168-6445(03)00046-9.

Beckers, F., Rinklebe, J., 2017. Cycling of mercury in the environment: sources, fate, and human health implications: a review. Crit. Rev. Environ. Sci. Technol. 47, 693–794. https://doi.org/10.1080/10643389.2017.1326277.

Bełdowska, M., Kobos, J., 2016. Mercury concentration in phytoplankton in response to warming of an autumn - winter season. Environ. Pollut. 215, 38–47. https://doi.org/10.1016/j.envpol.2016.05.002.

Bettoso, N., Pittaluga, F., Predonzani, S., Zanello, A., Acquavita, A., 2023. Mercury levels in sediment, water and selected organisms collected in a coastal contaminated environment: the Marano and Grado Lagoon (Northern Adriatic Sea, Italy). Appl. Sci. 13, 3064. https://doi.org/10.3390/app13053064.

Black, F.J., Conaway, C.H., Flegal, A.R., 2009. Stability of dimethyl mercury in seawater and its conversion to monomethyl mercury. Environ. Sci. Technol. 43, 4056–4062. https://doi.org/10.1021/es9001218.

Boldrin, A., Carniel, S., Giani, M., Marini, M., Bernardi Aubry, F., Campanelli, A., Grilli, F., Russo, A., 2009. Effects of bora wind on physical and biogeochemical properties of stratified waters in the northern Adriatic. J. Geophys. Res. 114, C08S92. https://doi.org/10.1029/2008jc004837.

Bouchet, S., Tessier, E., Monperrus, M., Bridou, R., Clavier, J., Thouzeau, G., Amouroux, D., 2011. Measurements of gaseous mercury exchanges at the sediment-water, water-atmosphere and sediment-atmosphere interfaces of a tidal environment (Arcachon Bay, France). J. Environ. Monit. 13, 1351–1359. https://doi.org/10.1039/c0em00358a.

Bouffard, A., Amyot, M., 2009. Importance of elemental mercury in lake sediments. Chemosphere 74, 1098–1103. https://doi.org/10.1016/j.chemosphere.2008.10.045.

Branfireun, B.A., Cosio, C., Poulain, A.J., Riise, G., Bravo, A.G., 2020. Mercury cycling in freshwater systems - an updated conceptual model. Sci. Total Environ. 745, 140906 https://doi.org/10.1016/j.scitotenv.2020.140906.

Bratkič, A., Ogrinc, N., Kotnik, J., Faganeli, J., Žagar, D., Yano, S., Tada, A., Horvat, M., 2013. Mercury speciation driven by seasonal changes in a contaminated estuarine environment. Environ. Res. 125, 171–178. https://doi.org/10.1016/j.envres.2013.01.004.

Bratkič, A., Tinta, T., Koron, N., Guevara, S.R., Begu, E., Barkay, T., Horvat, M., Falnoga, I., Faganeli, J., 2018. Mercury transformations in a coastal water column (Gulf of Trieste, northern Adriatic Sea). Mar. Chem. 200, 57–67. https://doi.org/10.1016/j.marchem.2018.01.001.

Castelle, S., Schäfer, J., Blanc, G., Dabrin, A., Lanceleur, L., Masson, M., 2009. Gaseous mercury at the air-water interface of a highly turbid estuary (Gironde Estuary, France). Mar. Chem. 117, 42–51. https://doi.org/10.1016/j.marchem.2009.01.005.

Castro, L., Dommergue, A., Larose, C., Ferrari, C., Maron, L., 2011. A Theoretical study of abiotic methylation reactions of gaseous elemental mercury by halogen-containing molecules. J. Phys. Chem. A 115, 5602–5608. https://doi.org/10.1021/jp200643n.

Cesário, R., Hintelmann, H., O'Driscoll, N.J., Monteiro, C.E., Caetano, M., Nogueira, M., Mota, A.M., Canário, J., 2017a. Biogeochemical cycle of mercury and methylmercury in two highly contaminated areas of Tagus estuary (Portugal). Water. Air. Soil Pollut 228, 257. https://doi.org/10.1007/s11270-017-3442-1.

Cesário, R., Poissant, L., Pilote, M., O'Driscoll, N.J., Mota, A.M., Canário, J., 2017b. Dissolved gaseous mercury formation and mercury volatilization in intertidal sediments. Sci. Total Environ. 603–604, 279–289. https://doi.org/10.1016/j.scitotenv.2017.06.093.

Chen, Y.S., Tseng, C.M., Reinfelder, J.R., 2020. Spatiotemporal variations in dissolved elemental mercury in the river-dominated and monsoon-influenced east China sea: drivers, budgets, and implications. Environ. Sci. Technol. 54, 3988–3995. https://doi.org/10.1021/acs.est.9b06092.

Cheng, G., Li, D., Li, Y., 2019. Distribution of dissolved gaseous mercury (DGM)and its controlling factors in the Yellow Sea and Bohai Sea. Ecotoxicol. Environ. Saf. 180, 715–722. https://doi.org/10.1016/j.ecoenv.2019.05.049.

Ci, Z., Zhang, X., Yin, Y., Chen, J., Wang, S., 2016. Mercury redox chemistry in waters of the eastern asian seas: from polluted coast to clean open ocean. Environ. Sci. Technol. 50, 2371–2380. https://doi.org/10.1021/acs.est.5b05372.

Ci, Z.J., Zhang, X.S., Wang, Z.W., Niu, Z.C., Diao, X.Y., Wang, S.W., 2011. Distribution and air-sea exchange of mercury (Hg) in the Yellow Sea. Atmos. Chem. Phys. 11, 2881–2892. https://doi.org/10.5194/acp-11-2881-2011.

Cizdziel, J.V., Zhang, Y., Nallamothu, D., Brewer, J.S., Gao, Z., 2019. Air/surface exchange of gaseous elemental mercury at different landscapes in Mississippi. Atmosphere 10, 538. https://doi.org/10.3390/atmos10090538. USA.

Clarke, R.G., Klapstein, S.J., Keenan, R., O'Driscoll, N.J., 2023. Mercury photoreduction and photooxidation kinetics in estuarine water: effects of salinity and dissolved organic matter. Chemosphere 312, 137279. https://doi.org/10.1016/j.chemosphere.2022.137279.

Colombo, M.J., Ha, J., Reinfelder, J.R., Barkay, T., Yee, N., 2013. Anaerobic oxidation of Hg(0) and methylmercury formation by Desulfovibrio desulfuricans ND132. Geochem. Cosmochim. Acta 112, 166–177. https://doi.org/10.1016/j.gca.2013.03.001.

Conaway, C.H., Squire, S., Mason, R.P., Flegal, A.R., 2003. Mercury speciation in the san Francisco bay estuary. Mar. Chem. 80, 199–225. https://doi.org/10.1016/S0304-4203(02)00135-4.

Cossa, D., Averty, B., Pirrone, N., 2009. The origin of methylmercury in open mediterranean waters. Limnol. Oceanogr. 54, 837–844. https://doi.org/10.4319/lo.2009.54.3.0837.

Cossa, D., Knoery, J., Bănaru, D., Harmelin-Vivien, M., Sonke, J.E., Hedgecock, I.M., Bravo, A.G., Rosati, G., Canu, D., Horvat, M., Sprovieri, F., Pirrone, N., Heimbürger-Boavida, L.E., 2022. Mediterranean mercury assessment 2022: an updated budget, health consequences, and research perspectives. Environ. Sci. Technol. 56, 3840–3862. https://doi.org/10.1021/acs.est.1c03044.

Costa, M., Liss, P.S., 1999. Photoreduction of mercury in sea water and its possible implications for Hg0 air-sea fluxes. Mar. Chem. 68, 87–95. https://doi.org/10.1016/S0304-4203(99)00067-5.

Covelli, S., Acquavita, A., Piani, R., Predonzani, S., De Vittor, C., 2009. Recent contamination of mercury in an estuarine environment (Marano lagoon, Northern Adriatic, Italy). Estuar. Coast Shelf Sci. 82, 273–284. https://doi.org/10.1016/j.ecss.2009.01.021.

Covelli, S., Faganeli, J., De Vittor, C., Predonzani, S., Acquavita, A., Horvat, M., 2008. Benthic fluxes of mercury species in a lagoon environment (Grado lagoon, northern Adriatic Sea, Italy). Appl. Geochem. 23, 529–546. https://doi.org/10.1016/j.apgeochem.2007.12.011.

Covelli, S., Faganeli, J., Horvat, M., Brambati, A., 2001. Mercury contamination of coastal sediments as the result of long-term cinnabar mining activity (Gulf of Trieste, northern Adriatic sea). Appl. Geochem. 16, 541–558. https://doi.org/10.1016/S0883-2927(00)00042-1.

Covelli, S., Piani, R., Acquavita, A., Predonzani, S., Faganeli, J., 2007. Transport and dispersion of particulate Hg associated with a river plume in coastal Northern Adriatic environments. Mar. Pollut. Bull. 55, 436–450. https://doi.org/10.1016/j.marpolbul.2007.09.006.

Covelli, S., Piani, R., Kotnik, J., Horvat, M., Faganeli, J., Brambati, A., 2006. Behaviour of Hg species in a microtidal deltaic system: the Isonzo River mouth (northern Adriatic Sea). Sci. Total Environ. 368, 210–223. https://doi.org/10.1016/j.scitotenv.2005.09.089.

Cozzi, S., Falconi, C., Comici, C., Čermelj, B., Kovac, N., Turk, V., Giani, M., 2012. Recent evolution of river discharges in the Gulf of Trieste and their potential response to climate changes and anthropogenic pressure. Estuar. Coast Shelf Sci. 115, 14–24. https://doi.org/10.1016/j.ecss.2012.03.005.

Custodio, D., Ebinghaus, R., Gerard Spain, T., Bieser, J., 2020. Source apportionment of atmospheric mercury in the remote marine atmosphere: mace Head GAW station, Irish western coast. Atmos. Chem. Phys. 20, 7929–7939. https://doi.org/10.5194/acp-20-7929-2020.

De Vittor, C., Faganeli, J., Emili, A., Covelli, S., Predonzani, S., Acquavita, A., 2012. Benthic fluxes of oxygen, carbon and nutrients in the Marano and Grado lagoon (northern Adriatic Sea, Italy). Estuar. Coast Shelf Sci. 113, 57–70. https://doi.org/10.1016/j.ecss.2012.03.031.

Díez, S., 2009. In: Whitacre, D.M. (Ed.), Human Health Effects of Methylmercury Exposure BT - Reviews of Environmental Contamination and Toxicology. Springer New York, New York, NY, pp. 111–132. https://doi.org/10.1007/978-0-387-09647-6_3.

Dizdarevič, T., 2001. The influence of mercury production in Idrija mine on the environment in the Idrija region and over a broad area. RMZ Mater. Geoenviron 48, 56–64.

Eckley, C.S., Gustin, M., Lin, C.J., Li, X., Miller, M.B., 2010. The influence of dynamic chamber design and operating parameters on calculated surface-to-air mercury fluxes. Atmos. Environ. 44, 194–203. https://doi.org/10.1016/j.atmosenv.2009.10.013.

Eckley, C.S., Hintelmann, H., 2006. Determination of mercury methylation potentials in the water column of lakes across Canada. Sci. Total Environ. 368, 111–125. https://doi.org/10.1016/j.scitotenv.2005.09.042.

Emili, A., Acquavita, A., Koron, N., Covelli, S., Faganeli, J., Horvat, M., Žižek, S., Fajon, V., 2012. Benthic flux measurements of Hg species in a northern Adriatic lagoon environment (Marano and Grado Lagoon, Italy). Estuar. Coast Shelf Sci. 113, 71–84. https://doi.org/10.1016/j.ecss.2012.05.018.

Enrico, M., Le Roux, G., Heimbürger, L.E., Van Beek, P., Souhaut, M., Chmeleff, J., Sonke, J.E., 2017. Holocene atmospheric mercury levels reconstructed from peat bog mercury stable isotopes. Environ. Sci. Technol. 51, 5899–5906. https://doi.org/10.1021/acs.est.6b05804.

Faganeli, J., Horvat, M., Covelli, S., Fajon, V., Logar, M., Lipej, L., Cermelj, B., 2003. Mercury and methylmercury in the Gulf of Trieste (northern Adriatic Sea). Sci. Total Environ. 304, 315–326. https://doi.org/10.1016/S0048-9697(02)00578-8.

Faganeli, J., Planinc, R., Pezdič, Smodiš, B., Stegnar, P., Ogorelec, B., 1991. Marine geology of the Gulf of Trieste (northern adriatic): geochemical aspects. Mar. Geol. 99, 93–108. https://doi.org/10.1016/0025-3227(91)90085-I.

Fantozzi, L., Ferrara, R., Frontini, F.P., Dini, F., 2009. Dissolved gaseous mercury production in the dark: evidence for the fundamental role of bacteria in different types of Mediterranean water bodies. Sci. Total Environ. 407, 917–924. https://doi.org/10.1016/j.scitotenv.2008.09.014.

Fantozzi, L., Ferrara, R., Frontini, F.P., Dini, F., 2007. Factors influencing the daily behaviour of dissolved gaseous mercury concentration in the Mediterranean Sea. Mar. Chem. 107, 4–12. https://doi.org/10.1016/j.marchem.2007.02.008.

Fantozzi, L., Manca, G., Ammoscato, I., Pirrone, N., Sprovieri, F., 2013. The cycling and sea-air exchange of mercury in the waters of the Eastern Mediterranean during the 2010 MED-OCEANOR cruise campaign. Sci. Total Environ. 448, 151–162. https://doi.org/10.1016/j.scitotenv.2012.09.062.

Ferrara, R., Mazzolai, B., 1998. A dynamic flux chamber to measure mercury emission from aquatic systems. Sci. Total Environ. 215, 51–57. https://doi.org/10.1016/S0048-9697(98)00117-X.

Ferrara, R., Mazzolai, B., Lanzillotta, E., Nucaro, E., Pirrone, N., 2000. Temporal trends in gaseous mercury evasion from the Mediterranean seawaters. Sci. Total Environ. 259, 183–190. https://doi.org/10.1016/S0048-9697(00)00581-7.

Ferrarin, C., Umgiesser, G., Bajo, M., Bellafiore, D., De Pascalis, F., Ghezzo, M., Mattassi, G., Scroccaro, I., 2010. Hydraulic zonation of the lagoons of Marano and Grado, Italy. A modelling approach. Estuar. Coast Shelf Sci. 87, 561–572. https://doi.org/10.1016/j.ecss.2010.02.012.

Fitzgerald, W.F., Engstrom, D.R., Mason, R.P., Nater, E.A., 1998. The case for atmospheric mercury contamination in remote areas. Environ. Sci. Technol. 32, 1–7. https://doi.org/10.1021/es970284w.

Fitzgerald, W.F., Lamborg, C.H., Hammerschmidt, C.R., 2007. Marine biogeochemical cycling of mercury. Chem. Rev. 107, 641–662. https://doi.org/10.1021/cr050353m.

Floreani, F., Acquavita, A., Barago, N., Klun, K., Faganeli, J., Covelli, S., 2022. Gaseous mercury exchange from water – air interface in differently impacted freshwater environments. Int. J. Environ. Res. Publ. Health 19, 8149. https://doi.org/10.3390/ijerph191381499.

Floreani, F., Acquavita, A., Petranich, E., Covelli, S., 2019. Diurnal fluxes of gaseous elemental mercury from the water-air interface in coastal environments of the northern Adriatic Sea. Sci. Total Environ. 668, 925–935. https://doi.org/10.1016/j.scitotenv.2019.03.012.

Floreani, F., Barago, N., Acquavita, A., Covelli, S., Skert, N., Higueras, P., 2020. Spatial distribution and biomonitoring of atmospheric mercury concentrations over a contaminated coastal lagoon (Northern Adriatic, Italy). Atmosphere 11, 1280. https://doi.org/10.3390/atmos11121280.

Fu, X., Feng, X., Zhang, G., Xu, W., Li, X., Yao, H., Liang, P., Li, J., Sommar, J., Yin, R., Liu, N., 2010. Mercury in the marine boundary layer and seawater of the South China Sea: concentrations, sea/air flux, and implication for land outflow. J. Geophys. Res. Atmos. 115, 1–11. https://doi.org/10.1029/2009JD012958.

Garcia, E., Poulain, A.J., Amyot, M., Ariya, P.A., 2005. Diel variations in photoinduced oxidation of Hg0 in freshwater. Chemosphere 59, 977–981. https://doi.org/10.1016/j.chemosphere.2004.09.107.

Gårdfeldt, K., Feng, X., Sommar, J., Lindqvist, O., 2001. Total gaseous mercury exchange between air and water at river and sea surfaces in Swedish coastal regions. Atmos. Environ. 35, 3027–3038. https://doi.org/10.1016/S1352-2310(01)00106-6.

Gårdfeldt, K., Sommar, J., Ferrara, R., Ceccarini, C., Lanzillotta, E., Munthe, J., Wängberg, I., Lindqvist, O., Pirrone, N., Sprovieri, F., Pesenti, E., Strömberg, D., 2003. Evasion of mercury from coastal and open waters of the atlantic ocean and the Mediterranean Sea. Atmos. Environ. 37, 73–84. https://doi.org/10.1016/S1352-2310(03)00238-3.

Gonzalez-Raymat, H., Liu, G., Liriano, C., Li, Y., Yin, Y., Shi, J., Jiang, G., Cai, Y., 2017. Elemental mercury: its unique properties affect its behavior and fate in the environment. Environ. Pollut. 229, 69–86. https://doi.org/10.1016/j.envpol.2017.04.101.

Gosar, M., Pirc, S., Bidovec, M., 1997. Mercury in the Idrijca River sediments as a reflection of mining and smelting activities of the Idrija mercury mine. J. Geochem. Explor. 58, 125–131. https://doi.org/10.1016/S0375-6742(96)00064-7.

Grégoire, D.S., Poulain, A.J., 2014. A little bit of light goes a long way: the role of phototrophs on mercury cycling. Metallomics 6, 396–407. https://doi.org/10.1039/c3mt00312d.

Hammerschmidt, C.R., Fitzgerald, W.F., 2004. Geochemical controls on the production and distribution of methylmercury in near-shore marine sediments. Environ. Sci. Technol. 38, 1487–1495. https://doi.org/10.1021/es034528q.

He, F., Zhao, W., Liang, L., Gu, B., 2014. Photochemical oxidation of dissolved elemental mercury by carbonate radicals in water. Environ. Sci. Technol. Lett. 1, 499–503. https://doi.org/10.1021/ez500322f.

Hines, M.E., Covelli, S., Faganeli, J., Horvat, M., 2017. Controls on microbial mercury transformations in contaminated sediments downstream of the Idrija mercury mine (West Slovenia) to the Gulf of Trieste (northern Adriatic). J. Soils Sediments 17, 1961–1971. https://doi.org/10.1007/s11368-016-1616-x.

Horvat, M., Kotnik, J., Logar, M., Fajon, V., Zvonarić, T., Pirrone, N., 2003. Speciation of mercury in surface and deep-sea waters in the Mediterranean Sea. Atmos. Environ. 37, 93–108. https://doi.org/10.1016/S1352-2310(03)00249-8.

Hsu-Kim, H., Eckley, C.S., Achá, D., Feng, X., Gilmour, C.C., Jonsson, S., Mitchell, C.P.J., 2018. Challenges and opportunities for managing aquatic mercury pollution in altered landscapes. Ambio 47, 141–169. https://doi.org/10.1007/s13280-017-1006-7.

Jung, E., Kim, H., Yun, D., Rahman, M.M., Lee, J.H., Kim, S., Kim, C.K., Han, S., 2022. Importance of hydraulic residence time for methylmercury accumulation in sediment and fish from artificial reservoirs. Chemosphere 293, 133545. https://doi.org/10.1016/j.chemosphere.2022.133545.

Kalinchuk, V.V., 2023. Gaseous elemental mercury and its evasion fluxes in the marine boundary layer of the marginal seas of the northwestern Pacific: results from two cruises in September–December 2019. Sci. Total Environ. 858, 159711 https://doi.org/10.1016/j.scitotenv.2022.159711.

Kalinchuk, V.V., Lopatnikov, E.A., Astakhov, A.S., Ivanov, M.V., Hu, L., 2021. Distribution of atmospheric gaseous elemental mercury (Hg(0)) from the Sea of Japan to the Arctic, and Hg(0) evasion fluxes in the Eastern Arctic Seas: results from a joint Russian-Chinese cruise in fall 2018. Sci. Total Environ. 753, 142003 https://doi.org/10.1016/j.scitotenv.2020.142003.

Klapstein, S.J., O'Driscoll, N.J., 2018. Methylmercury biogeochemistry in freshwater ecosystems: a review focusing on DOM and photodemethylation. Bull. Environ. Contam. Toxicol. 100, 14–25. https://doi.org/10.1007/s00128-017-2236-x.

Kotnik, J., Horvat, M., Begu, E., Shlyapnikov, Y., Sprovieri, F., Pirrone, N., 2017. Dissolved gaseous mercury (DGM) in the Mediterranean Sea: spatial and temporal trends. Mar. Chem. 193, 8–19. https://doi.org/10.1016/j.marchem.2017.03.002.

Kotnik, J., Horvat, M., Ogrinc, N., Fajon, V., Žagar, D., Cossa, D., Sprovieri, F., Pirrone, N., 2015. Mercury speciation in the Adriatic Sea. Mar. Pollut. Bull. 96, 136–148. https://doi.org/10.1016/j.marpolbul.2015.05.037.

Kotnik, J., Žagar, D., Novak, G., Ličer, M., Horvat, M., 2022. Dissolved gaseous mercury (DGM) in the Gulf of Trieste, northern Adriatic Sea. J. Mar. Sci. Eng. 10, 587. https://doi.org/10.3390/jmse10050587.

Kuss, J., Holzmann, J., Ludwig, R., 2009. An elemental mercury diffusion coefficient for natural waters determined by molecular dynamics simulation. Environ. Sci. Technol. 43, 3183–3186. https://doi.org/10.1021/es8034889.

Kuss, J., Krüger, S., Ruickoldt, J., Wlost, K.P., 2018. High-resolution measurements of elemental mercury in surface water for an improved quantitative understanding of the Baltic Sea as a source of atmospheric mercury. Atmos. Chem. Phys. 18, 4361–4376. https://doi.org/10.5194/acp-18-4361-2018.

Kuss, J., Wasmund, N., Nausch, G., Labrenz, M., 2015. Mercury emission by the baltic sea: a consequence of cyanobacterial activity, photochemistry, and low-light mercury transformation. Environ. Sci. Technol. 49, 11449–11457. https://doi.org/10.1021/acs.est.5b02204.

Lalonde, J.D., Amyot, M., Kraepiel, A.M.L., Morel, F.M.M., 2001. Photooxidation of Hg (O) in artificial and natural waters. Environ. Sci. Technol. 35, 1367–1372. https://doi.org/10.1021/es001408z.

Lalonde, J.D., Amyot, M., Orvoine, J., Morel, F.M.M., Auclair, J.C., Ariya, P.A., 2004. Photoinduced oxidation of Hg0(aq) in the waters from the St. Lawrence estuary. Environ. Sci. Technol. 38, 508–514. https://doi.org/10.1021/es034394g.

Lamborg, C.H., Hansel, C.M., Bowman, K.L., Voelker, B.M., Marsico, R.M., Oldham, V.E., Swarr, G.J., Zhang, T., Ganguli, P.M., 2021. Dark reduction drives evasion of mercury from the ocean. Front. Environ. Chem. 2, 659085 https://doi.org/10.3389/fenvc.2021.659085.

Lanzillotta, E., Ceccarini, C., Ferrara, R., 2002. Photo-induced formation of dissolved gaseous mercury in coastal and offshore seawater of the Mediterranean basin. Sci. Total Environ. 300, 179–187. https://doi.org/10.1016/S0048-9697(02)00223-1.

Lanzillotta, E., Ceccarini, C., Ferrara, R., Dini, F., Frontini, F.P., Banchetti, R., 2004. Importance of the biogenic organic matter in photo-formation of dissolved gaseous mercury in a culture of the marine diatom Chaetoceros sp. Sci. Total Environ. 318, 211–221. https://doi.org/10.1016/S0048-9697(03)00400-5.

Lee, J.I., Yang, J.H., Kim, P.R., Han, Y.J., 2019. Effects of organic carbon and UV wavelength on the formation of dissolved gaseous mercury in water under a controlled environment. Environ. Eng. Res. 24, 54–62. https://doi.org/10.4491/eer.2018.045.

Lepak, R.F., Tate, M.T., Ogorek, J.M., DeWild, J.F., Peterson, B.D., Hurley, J.P., Krabbenhoft, D.P., 2021. Aqueous elemental mercury production versus mercury inventories in the lake Michigan airshed: deciphering the spatial and diel controls of mercury gradients in air and water. ACS ES&T Water 1, 719–727. https://doi.org/10.1021/acsestwater.0c00187.

Liang, X., Zhu, N., Johs, A., Chen, H., Pelletier, D.A., Zhang, L., Yin, X., Gao, Y., Zhao, J., Gu, B., 2022. Mercury reduction, uptake, and species transformation by freshwater alga chlorella vulgaris under sunlit and dark conditions. Environ. Sci. Technol. https://doi.org/10.1021/acs.est.1c06558.

Lindberg, S.E., Zhang, H., 2000. Air/water exchange of mercury in the Everglades II: measuring and modeling evasion of mercury from surface waters in the Everglades Nutrient Removal Project. Sci. Total Environ. 259, 135–143. https://doi.org/10.1016/S0048-9697(00)00586-6.

Lindberg, S.I.S., Meyers, T.P., 1995. Evasion of mercury vapor from the surface of a recently limed acid lake forest in Sweden. Water. Air. Soil Pollut 85, 725–730.

Luo, H., Cheng, Q., Pan, X., 2020. Photochemical behaviors of mercury (Hg) species in aquatic systems: a systematic review on reaction process, mechanism, and influencing factor. Sci. Total Environ. 720, 137540 https://doi.org/10.1016/j.scitotenv.2020.137540.

Marumoto, K., Imai, S., 2015. Determination of dissolved gaseous mercury in seawater of Minamata Bay and estimation for mercury exchange across air-sea interface. Mar. Chem. 168, 9–17. https://doi.org/10.1016/j.marchem.2014.09.007.

Mason, R.P., Hammerschmidt, C.R., Lamborg, C.H., Bowman, K.L., Swarr, G.J., Shelley, R.U., 2017. The air-sea exchange of mercury in the low latitude Pacific and Atlantic Oceans. Deep. Res. Part I Oceanogr. Res. Pap. 122, 17–28. https://doi.org/10.1016/j.dsr.2017.01.015.

Mason, R.P., Morel, F.M.M., Hemond, H.F., 1995. The role of microorganisms in elemental mercury formation in natural waters. Water, Air. Soil Pollut 80, 775–787. https://doi.org/10.1007/BF01189729.

Mason, R.P., Sheu, G.R., 2002. Role of the ocean in the global mercury cycle. Global Biogeochem. Cycles 16, 40–41. https://doi.org/10.1029/2001gb001440, 40–14.

Millard, G., Eckley, C.S., Luxton, T.P., Krabbenhoft, D., Goetz, J., McKernan, J., DeWild, J., 2023. Evaluating the influence of seasonal stratification on mercury methylation rates in the water column and sediment in a contaminated section of a western U.S.A. reservoir. Environ. Pollut. 316, 120485 https://doi.org/10.1016/j.envpol.2022.120485.

Monperrus, M., Tessier, E., Point, D., Vidimova, K., Amouroux, D., Guyoneaud, R., Leynaert, A., Grall, J., Chauvaud, L., Donard, O.F.X., 2007. The biogeochemistry of mercury at the sediment-water interface in the Thau Lagoon. 2. Evaluation of mercury methylation potential in both surface sediment and water column. Estuar. Coast Shelf Sci. 72, 485–496. https://doi.org/10.1016/j.ecss.2006.11.014.

Morel, F.M.M., Kraepiel, A.M.L., Amyot, M., 1998. The chemical cycle and bioaccumulation of mercury. Annu. Rev. Ecol. Systemat. 29, 543–566. https://doi.org/10.1146/annurev.ecolsys.29.1.543.

Narukawa, M., Sakata, M., Marumoto, K., Asakura, K., 2006. Air-sea exchange of mercury in Tokyo Bay. J. Oceanogr. 62, 249–257. https://doi.org/10.1007/s10872-006-0049-3.

Nerentorp Mastromonaco, M.G., Gårdfeldt, K., Wängberg, I., 2017. Seasonal and spatial evasion of mercury from the western Mediterranean Sea. Mar. Chem. 193, 34–43. https://doi.org/10.1016/j.marchem.2017.02.003.

O'Driscoll, N.J., Beauchamp, S., Siciliano, S.D., Rencz, A.N., Lean, D.R.S., 2003. Continuous analysis of dissolved gaseous mercury (DGM) and mercury flux in two freshwater lakes in Kejimkujik Park, Nova Scotia: Evaluating mercury flux models with quantitative data. Environ. Sci. Technol. 37, 2226–2235. https://doi.org/10.1021/es025944y.

O'Driscoll, N.J., Christensen, T.M., Mann, E.A., Keenan, R., Klapstein, S.J., 2022. Temporal Changes in Photoreducible Mercury, Photoreduction Rates, and the Role of Dissolved Organic Matter in Freshwater Lakes. Bull. Environ. Contam. Toxicol. 108, 635–640. https://doi.org/10.1007/s00128-021-03422-1.

O'Driscoll, N.J., Covelli, S., Petranich, E., Floreani, F., Klapstein, S., Acquavita, A., 2019. Dissolved Gaseous Mercury Production at a Marine Aquaculture Site in the Mercury-Contaminated Marano and Grado Lagoon. Italy. Bull. Environ. Contam. Toxicol. 103 https://doi.org/10.1007/s00128-019-02621-1.

O'Driscoll, N.J., Lean, D.R.S., Loseto, L.L., Carignan, R., Siciliano, S.D., 2004. Effect of Dissolved Organic Carbon on the Photoproduction of Dissolved Gaseous Mercury in Lakes: Potential Impacts of Forestry. Environ. Sci. Technol. 38, 2664–2672. https://doi.org/10.1021/es034702a.

O'Driscoll, N.J., Vost, E., Mann, E., Klapstein, S., Tordon, R., Lukeman, M., 2018. Mercury photoreduction and photooxidation in lakes: Effects of filtration and dissolved organic carbon concentration. J. Environ. Sci. (China) 68, 151–159. https://doi.org/10.1016/j.jes.2017.12.010.

Ogorelec, B., Mišič, M., Faganeli, J., 1991. Marine geology of the Gulf of Trieste (northern Adriatic): Sedimentological aspects. Mar. Geol. 99, 79–92. https://doi.org/10.1016/0025-3227(91)90084-H.

Osterwalder, S., Nerentorp, M., Zhu, W., Jiskra, M., Nilsson, E., Nilsson, M.B., Rutgersson, A., Soerensen, A.L., Sommar, J., Wallin, M.B., Wängberg, I., Bishop, K., 2021. Critical Observations of Gaseous Elemental Mercury Air-Sea Exchange. Global Biogeochem. Cycles 35, e2020GB006742. https://doi.org/10.1029/2020GB006742.

Parks, J.M., Johs, A., Podar, M., Bridou, R., Hurt, R.A., Smith, S.D., Tomanicek, S.J., Qian, Y., Brown, S.D., Brandt, C.C., Palumbo, A.V., Smith, J.C., Wall, J.D., Elias, D. A., Liang, L., 2013. The genetic basis for bacterial mercury methylation. Science (80-339, 1332–1335. https://doi.org/10.1126/science.1230667.

Pavoni, E., Crosera, M., Petranich, E., Oliveri, P., Klun, K., Faganeli, J., Covelli, S., Adami, G., 2020. Trace elements in the estuarine systems of the Gulf of Trieste (northern Adriatic Sea): A chemometric approach to depict partitioning and behaviour of particulate, colloidal and truly dissolved fractions. Chemosphere 252, 126517. https://doi.org/10.1016/j.chemosphere.2020.126517.

Pesaresi, S., Galdenzi, D., Biondi, E., Casavecchia, S., 2014. Bioclimate of Italy: Application of the worldwide bioclimatic classification system. J. Maps 10, 538–553. https://doi.org/10.1080/17445647.2014.891472.

Petranich, E., Covelli, S., Acquavita, A., De Vittor, C., Faganeli, J., Contin, M., 2018a. Benthic nutrient cycling at the sediment-water interface in a lagoon fish farming system (northern Adriatic Sea, Italy). Sci. Total Environ. 644, 137–149. https://doi.org/10.1016/j.scitotenv.2018.06.310.

Petranich, E., Covelli, S., Acquavita, A., Faganeli, J., Horvat, M., Contin, M., 2018b. Evaluation of mercury biogeochemical cycling at the sediment–water interface in anthropogenically modified lagoon environments. J. Environ. Sci. (China) 68, 5–23. https://doi.org/10.1016/j.jes.2017.11.014.

Poissant, L., Amyot, M., Pilote, M., Lean, D., 2000. Mercury water - Air exchange over the upper St. Lawrence River and Lake Ontario. Environ. Sci. Technol. 34, 3069–3078. https://doi.org/10.1021/es990719a.

Poulain, A.J., Amyot, M., Findlay, D., Telor, S., Barkay, T., Hintelmann, H., 2004. Biological and photochemical production of dissolved gaseous mercury in a boreal lake. Limnol. Oceanogr. 49, 2265–2275. https://doi.org/10.4319/lo.2004.49.6.2265.

Qureshi, A., O'Driscoll, N.J., Macleod, M., Neuhold, Y.M., Hungerbühler, K., 2010. Photoreactions of mercury in surface ocean water: Gross reaction kinetics and possible pathways. Environ. Sci. Technol. 44, 644–649. https://doi.org/10.1021/es9012728.

Ren, X., Luke, W.T., Kelley, P., Cohen, M.D., Artz, R., Olson, M.L., Schmeltz, D., Puchalski, M., Goldberg, D.L., Ring, A., Mazzuca, G.M., Cummings, K.A., Wojdan, L., Preaux, S., Stehr, J.W., 2016. Atmospheric mercury measurements at a suburban site in the Mid-Atlantic United States: Inter-annual, seasonal and diurnal variations and source-receptor relationships. Atmos. Environ. 146, 141–152. https://doi.org/10.1016/j.atmosenv.2016.08.028.

Rolfhus, K.R., Fitzgerald, W.F., 2001. The evasion and spatial/temporal distribution of mercury species in Long Island Sound, CT-NY. Geochem. Cosmochim. Acta 65, 407–418. https://doi.org/10.1016/S0016-7037(00)00519-6.

Saiz-Lopez, A., Sitkiewicz, S.P., Roca-Sanjuán, D., Oliva-Enrich, J.M., Dávalos, J.Z., Notario, R., Jiskra, M., Xu, Y., Wang, F., Thackray, C.P., Sunderland, E.M., Jacob, D. J., Travnikov, O., Cuevas, C.A., Acuña, A.U., Rivero, D., Plane, J.M.C., Kinnison, D. E., Sonke, J.E., 2018. Photoreduction of gaseous oxidized mercury changes global atmospheric mercury speciation, transport and deposition. Nat. Commun. 9, 4796. https://doi.org/10.1038/s41467-018-07075-3.

Sanemasa, I., 1975. The solubility of elemental mercury vapor in water. Bull. Chem. Soc. Jpn. 48, 1795–1798.

Schartup, A.T., Ndu, U., Balcom, P.H., Mason, R.P., Sunderland, E.M., 2015. Contrasting effects of marine and terrestrially derived dissolved organic matter on mercury speciation and bioavailability in seawater. Environ. Sci. Technol. 49, 5965–5972. https://doi.org/10.1021/es506274x.

Selin, H., Keane, S.E., Wang, S., Selin, N.E., Davis, K., Bally, D., 2018. Linking science and policy to support the implementation of the Minamata Convention on Mercury. Ambio 47, 198–215. https://doi.org/10.1007/s13280-017-1003-x.

Seller, P., Kelly, C.A., Rudd, J.W.M., Mac Hutchon, A.R., 1996. Photodegradation of methylmercury in lakes. Nature 380, 694–697. https://doi.org/10.1038/380694a0.

Sharif, A., Tessier, E., Bouchet, S., Monperrus, M., Pinaly, H., Amouroux, D., 2013. Comparison of different air-water gas exchange models to determine gaseous mercury evasion from different european coastal lagoons and estuaries. Water. Air. Soil Pollut. 224 https://doi.org/10.1007/s11270-013-1606-1.

Sholupov, S., Pogarev, S., Ryzhov, V., 2004. Zeeman atomic absorption spectrometer RA-915 + for direct determination of mercury in air and complex matrix samples 85, 473–485. https://doi.org/10.1016/j.fuproc.2003.11.003.

Soerensen, A.L., Mason, R.P., Balcom, P.H., Jacob, D.J., Zhang, Y., Kuss, J., Sunderland, E.M., 2014. Elemental mercury concentrations and fluxes in the tropical atmosphere and Ocean. Environ. Sci. Technol. 48, 11312–11319. https://doi.org/10.1021/es503109p.

Soerensen, A.L., Mason, R.P., Balcom, P.H., Sunderland, E.M., 2013. Drivers of surface ocean mercury concentrations and air-sea exchange in the West Atlantic Ocean. Environ. Sci. Technol. 47, 7757–7765. https://doi.org/10.1021/es401354q.

Soerensen, A.L., Sunderland, E.M., Holmes, C.D., Jacob, D.J., Yantosca, R.M., Skov, H., Christensen, J.H., Strode, S.A., Mason, R.P., 2010. An improved global model for air-sea exchange of mercury: High concentrations over the North Atlantic. Environ. Sci. Technol. 44, 8574–8580. https://doi.org/10.1021/es102032g.

Sommar, J., Osterwalder, S., Zhu, W., 2020. Recent advances in understanding and measurement of Hg in the environment: Surface-atmosphere exchange of gaseous elemental mercury (Hg0). Sci. Total Environ. 721, 137648 https://doi.org/10.1016/j.scitotenv.2020.137648.

Southworth, G., Lindberg, S., Hintelmann, H., Amyot, M., Poulain, A., Bogle, M.A., Peterson, M., Rudd, J., Harris, R., Sandilands, K., Krabbenhoft, D., Olsen, M., 2007. Evasion of added isotopic mercury from a northern temperate lake. Environ. Toxicol. Chem. 26, 53–60. https://doi.org/10.1897/06-148R.1.

Sprovieri, F., Pirrone, N., Bencardino, M., D'Amore, F., Angot, H., Barbante, C., Brunke, E.G., Arcega-Cabrera, F., Cairns, W., Comero, S., Del Carmen Diéguez, M., Dommergue, A., Ebinghaus, R., Bin Feng, X., Fu, X., Elizabeth Garcia, P., Manfred Gawlik, B., Hageström, U., Hansson, K., Horvat, M., Kotnik, J., Labuschagne, C., Magand, O., Martin, L., Mashyanov, N., Mkololo, T., Munthe, J., Obolkin, V., Ramirez Islas, M., Sena, F., Somerset, V., Spandow, P., Vardè, M., Walters, C., Wängberg, I., Weigelt, A., Yang, X., Zhang, H., 2017. Five-year records of mercury wet deposition flux at GMOS sites in the Northern and Southern hemispheres. Atmos. Chem. Phys. 17, 2689–2708. https://doi.org/10.5194/acp-17-2689-2017.

Sprovieri, F., Pirrone, N., Ebinghaus, R., Kock, H., Dommergue, A., 2010. A review of worldwide atmospheric mercury measurements. Atmos. Chem. Phys. 10, 8245–8265. https://doi.org/10.5194/acp-10-8245-2010.

Strode, S.A., Jaeglé, L., Selin, N.E., Jacob, D.J., Park, R.J., Yantosca, R.M., Mason, R.P., Slemr, F., 2007. Air-sea exchange in the global mercury cycle. Global Biogeochem. Cycles 21, 1–12. https://doi.org/10.1029/2006GB002766.

Sugimura, Y., Suzuki, Y., 1988. A high-temperature catalytic oxidation method for the determination of non-volatile dissolved organic carbon in seawater by direct injection of a liquid sample. Mar. Chem. 24, 105–131. https://doi.org/10.1016/0304-4203(88)90043-6.

Tomažič, Š., Ličer, M., Žagar, D., 2018. Numerical modelling of mercury evasion in a two-layered Adriatic Sea using a coupled atmosphere-ocean model. Mar. Pollut. Bull. 135, 1164–1173. https://doi.org/10.1016/j.marpolbul.2018.08.064.

Un Environment, 2019. Global Mercury Assessment 2018. UN Environment Programme. Chemicals and Health Branch, Geneva, Switzerland.

United States Environmental Protection Agency, 2002. Method 1631, Revision E: Mercury in Water by Oxidation, Purge and Trap, and Cold Vapor Atomic Fluorescence Spectrometry. Off. Water, Off. Sci. Technol. Eng. Anal. Div. 1200 (4303), 1–34. Pennsylvania Ave. NW, Washington, D.C.

United States Environmental Protection Agency Office of Environmental Information, 2000. Guidance for Data Quality Assessment: Practical Methods for Data Analysis EPA QA/G-9 QA00 UPDATE. U. S. Environmental Protection Agency Office, Washington, DC, USA.

Vette, A.F., Landis, M.S., Keeler, G.J., 2002. Deposition and emission of gaseous mercury to and from Lake Michigan during the Lake Michigan Mass Balance Study (July, 1994-October, 1995). Environ. Sci. Technol. 36, 4525–4532. https://doi.org/10.1021/es0112184.

Vudamala, K., Chakraborty, P., Sailaja, B.B.V., 2017. An insight into mercury reduction process by humic substances in aqueous medium under dark condition. Environ. Sci. Pollut. Res. 24, 14499–14507. https://doi.org/10.1007/s11356-017-8979-4.

Wang, C., Ci, Z., Wang, Z., Zhang, X., 2016. Air-sea exchange of gaseous mercury in the East China Sea. Environ. Pollut. 212, 535–543. https://doi.org/10.1016/j.envpol.2016.03.016.

Wang, C., He, L., Shi, X., Wei, S., Feng, X., 2006. Release flux of mercury from different environmental surfaces in Chongqing, China. Chemosphere 64, 1845–1854. https://doi.org/10.1016/j.chemosphere.2006.01.054.

Wang, C., Wang, Z., Zhang, X., 2020a. Characteristics of the air−sea exchange of gaseous mercury and deposition flux of atmospheric mercury at an island near the boundary of the Bohai Sea and Yellow Sea. Atmos. Environ. 232, 117547 https://doi.org/10.1016/j.atmosenv.2020.117547.

Wang, K., Liu, G., Cai, Y., 2022. Possible pathways for mercury methylation in oxic marine waters. Crit. Rev. Environ. Sci. Technol. 52, 3997–4015. https://doi.org/10.1080/10643389.2021.2008753.

Wang, Y., Li, Y., Liu, G., Wang, D., Jiang, G., Cai, Y., 2015. Elemental Mercury in Natural Waters: Occurrence and Determination of Particulate Hg(0). Environ. Sci. Technol. 49, 9742–9749. https://doi.org/10.1021/acs.est.5b01940.

Wang, Z., Fei, Z., Wu, Q., Yin, R., 2020b. Evaluation of the effects of Hg/DOC ratios on the reduction of Hg(II) in lake water. Chemosphere 253, 126634. https://doi.org/10.1016/j.chemosphere.2020.126634.

Wängberg, I., Munthe, J., Amouroux, D., Andersson, M.E., Fajon, V., Ferrara, R., Gårdfeldt, K., Horvat, M., Mamane, Y., Melamed, E., Monperrus, M., Ogrinc, N., Yossef, O., Pirrone, N., Sommar, J., Sprovieri, F., 2008. Atmospheric mercury at mediterranean coastal stations. Environ. Fluid Mech. 8, 101–116. https://doi.org/10.1007/s10652-007-9047-2.

Whalin, L., Kim, E.H., Mason, R., 2007. Factors influencing the oxidation, reduction, methylation and demethylation of mercury species in coastal waters. Mar. Chem. 107, 278–294. https://doi.org/10.1016/j.marchem.2007.04.002.

Wickham, H., Chang, W., Henry, L., Pendersen, T.L., Takahashi, K., Wilke, C., Woo, K., Yutani, H., Dunnington, D., 2016. ggplot2: Elegant Graphics for Data Analysis. Springer-Verlag, New York ggplot2.tidyverse.org.

Wu, Y., Wang, W.X., 2014. Intracellular speciation and transformation of inorganic mercury in marine phytoplankton. Aquat. Toxicol. 148, 122–129. https://doi.org/10.1016/j.aquatox.2014.01.005.

Xu, L.Q., Liu, R.H., Wang, J.Y., Tan, H.W., Tang, A.K., Yu, P., 2012. Mercury Emission Flux in the Jiaozhou Bay Measured by Flux Chamber. Procedia Environ. Sci. 13, 1500–1506. https://doi.org/10.1016/j.proenv.2012.01.142.

Xue, W., Kwon, S.Y., Grasby, S.E., Sunderland, E.M., Pan, X., Sun, R., Zhou, T., Yan, H., Yin, R., 2019. Anthropogenic influences on mercury in Chinese soil and sediment revealed by relationships with total organic carbon. Environ. Pollut. 255, 113186 https://doi.org/10.1016/j.envpol.2019.113186.

Yamamoto, M., 1996. Stimulation of elemental mercury oxidation in the presence of chloride ion in aquatic environments. Chemosphere 32, 1217–1224. https://doi.org/10.1016/0045-6535(96)00008-2.

Yin, Y., Li, Y., Tai, C., Cai, Y., Jiang, G., 2014. Fumigant methyl iodide can methylate inorganic mercury species in natural waters. Nat. Commun. 5, 4633. https://doi.org/10.1038/ncomms5633.

Zappa, C.J., Raymond, P.A., Terray, E.A., McGillis, W.R., 2003. Variation in Surface Turbulence and the Gas Transfer Velocity over a Tidal Cycle in a Macro-tidal Estuary. Estuaries 26, 1401–1415. https://doi.org/10.1007/BF02803649.

Zhang, L., Blanchard, P., Gay, D.A., Prestbo, E.M., Risch, M.R., Johnson, D., Narayan, J., Zsolway, R., Holsen, T.M., Miller, E.K., Castro, M.S., Graydon, J.A., St Louis, V.L., Dalziel, J., 2012. Estimation of speciated and total mercury dry deposition at monitoring locations in eastern and central North America. Atmos. Chem. Phys. 12, 4327–4340. https://doi.org/10.5194/acp-12-4327-2012.

Zhang, X., Guo, Y., Liu, G., Liu, Y., Song, M., Shi, J., Hu, L., Li, Y., Yin, Y., Cai, Y., Jiang, G., 2021. Dark Reduction of Mercury by Microalgae-Associated Aerobic Bacteria in Marine Environments. Environ. Sci. Technol. 55, 14258–14268. https://doi.org/10.1021/acs.est.1c03608.

Zheng, W., Hintelmann, H., 2009. Mercury isotope fractionation during photoreduction in natural water is controlled by its Hg/DOC ratio. Geochem. Cosmochim. Acta 73, 6704–6715. https://doi.org/10.1016/j.gca.2009.08.016.

Zhu, W., Lin, C.J., Wang, X., Sommar, J., Fu, X., Feng, X., 2016. Global observations and modeling of atmosphere-surface exchange of elemental mercury: A critical review. Atmos. Chem. Phys. 16, 4451–4480. https://doi.org/10.5194/acp-16-4451-2016.

Zhu, W., Sommar, J., Lin, C.J., Feng, X., 2015. Mercury vapor air-surface exchange measured by collocated micrometeorological and enclosure methods – Part I: Data comparability and method characteristics. Atmos. Chem. Phys. 15, 685–702. https://doi.org/10.5194/acp-15-685-2015.

Živković, I., Humphreys, M.P., Achterberg, E.P., Dumousseaud, C., Woodward, E.M.S., Bojanić, N., Šolić, M., Bratkič, A., Kotnik, J., Vahčič, M., Obu Vazner, K., Begu, E., Fajon, V., Shlyapnikov, Y., Horvat, M., 2022. Enhanced mercury reduction in the South Atlantic Ocean during carbon remineralization. Mar. Pollut. Bull. 178, 113644 https://doi.org/10.1016/j.marpolbul.2022.113644.